2

Monitoring Cell Calcium

Roger Y. Tsien

Significance

To understand cellular Ca^{2+}, one must be able to measure it. Cellular fluxes of Ca^{2+} bear some analogy to the flow of water in a plumbing system, the movement of charge in an electrical circuit, or even the distribution of goods in an economy. In each case, one needs to measure two distinct but related quantities, which for these examples are the water flow rate and the pressure, the electrical current and the voltage, or the quantity of goods and their unit price, respectively. For Ca^{2+}, the corresponding quantities are the concentration of total Ca^{2+} and the chemical potential of Ca^{2+}, which we would like to know in each relevant compartment of the cell. The chemical potential measures how much the thermodynamic free energy would change upon addition on an infinitesimal unit of Ca^{2+}. It therefore describes the "pressure" of Ca^{2+} or its propensity to drive Ca^{2+}-binding reactions. Most biologists find the chemical potential too abstract a parameter and prefer to think about and measure the free concentration of Ca^{2+}, perhaps because that has the familiar units of moles/liter. The chemical potential μ equals RT ln c, where R is the gas constant, T is the absolute temperature, and c is the free concentration, so the chemical potential and the free concentration carry the same information on logarithmic vs. linear scales. Newcomers to the field often wonder why we care about the free concentration, since, by definition, it measures the Ca^{2+} that is not bound, whereas the bound Ca^{2+} is what actually triggers biochemical responses. The answer to this query is that the free Ca^{2+} is just another way of expressing the local driving force available for Ca^{2+}-binding reactions in general (Campbell, 1983; Tsien, 1983). Naturally, the best way to measure free Ca^{2+} is to provide a sensitive reference reaction in which Ca^{2+} can participate and then measure how far the equilibrium proceeds.

Methods for Measuring Total Ca^{2+} or Ca^{2+} Fluxes

Methods for the absolute measurement of total cellular Ca^{2+} (Campbell, 1983) generally involve destruction of the tissue and liberation of bound Ca^{2+}. For example, the tissue can be ashed or extracted with acid. The Ca^{2+} content of the ash or extract is then determined by atomic absorption spectrophotometry, which measures the characteristic absorptions of vaporized calcium ions at extremely high temperatures in a flame or graphite furnace (Sanui and Rubin, 1982). Alternatively, if the tissue can be incubated with radioactive Ca^{2+} for long enough to reach tracer equilibrium, then scintillation counting of total radioactivity and specific activity yield the total cellular Ca^{2+}. Neither of these methods is used frequently nowadays, perhaps because cells usually contain large quantities of statically bound Ca^{2+}. Therefore, the changes in total Ca^{2+} that accompany signal transduction are usually buried in the experimental error, which includes variations in the amount of tissue in each successive sample.

Methods that measure *changes* of total Ca^{2+} as influx or efflux of Ca^{2+} across the plasma membrane are much more practical and common. If $^{45}Ca^{2+}$ is included in the bathing medium, unidirectional influxes can be measured as the initial rates of uptake of the isotropic tracer. Sequential samples of tissue must be taken and subjected to scintillation counting. The main technical problem is how to wash away, very rapidly, the large amount of radioactivity bound to the exterior of the cells without letting a significant amount of intracellular Ca^{2+} escape. Unidirectional effluxes may be measured by prelabeling the tissue to isotopic equilibrium, then counting the radioactivity released back into successive samples of supernatant medium. For many years, these techniques (see Borle, 1981, for a review) were among the most popular

types of experiments on cellular Ca^{2+}, perhaps because they require no specialized reagents or equipment. They are much less fashionable nowadays because they demand much skilled but repetitive manual manipulation of samples containing a short-lived hazardous isotope, and their spatial and temporal resolution is poor. Nevertheless, if unidirectional fluxes are to be quantified, isotopic methods are essential.

Several more methods are available for measuring *net* fluxes, especially across the plasma membrane. If the Ca^{2+} flows through channels whose ionic selectivity is known, measurement of the electrical current through the channel yields the flux of Ca^{2+}. Likewise, if a carrier or pump is electrogenic, if the stoichiometry of the transport cycle is known, and if the associated current can be resolved from all the other currents across the plasma membrane, then the flux is easily deduced. A good example is the resolution of a current component representing Na^+-Ca^{2+} exchange (Yau and Nakatani, 1984). However, in small nonexcitable cells, the currents associated with important Ca^{2+} influxes and effluxes are often minuscule and difficult to measure (Penner et al., 1988).

Another class of methods detects changes in extracellular free Ca^{2+} just outside the cell(s) under study; increases and decreases in extracellular free Ca^{2+} reflect net cellular extrusion and uptake, respectively. The extracellular concentration changes can be detected by low-affinity Ca^{2+} indicators of Ca^{2+}-selective electrodes. The fundamental difficulty in this approach is that the fractional change in extracellular free Ca^{2+} concentration is small. It can be increased by lowering the background level of Ca^{2+} so that cellular fluxes cause bigger percentage changes, though such low-Ca^{2+} media are likely to depress Ca^{2+} influxes. Decreasing the volume of extracellular medium being sampled, for example by pressing the cells against a Ca^{2+}-selective electrode or dispersing them in aqueous microdroplets under oil, is also necessary (Miller and Korenbrot, 1987; Tepikin et al., 1994; Belan et al., 1996). A Ca^{2+} indicator with an octadecyl tail, adsorbed to the outside of osteoblasts, is reported to detect hormone-stimulated Ca^{2+} efflux into a low-Ca^{2+} buffer (Lloyd et al., 1995). Mechanical vibration of Ca^{2+}-selective electrodes helps them to detect small local differences in extracellular Ca^{2+} next to sites of net Ca^{2+} uptake or extrusion (Smith et al., 1994). The tiny changes in electrode potential reflecting the local diffusion gradient of Ca^{2+} are synchronized with the mechanical motion of the electrode and can be selectively amplified to increase discrimination against random drift and noise.

A complementary strategy is to load the cell with a fluorescent indicator at a concentration high enough to become the dominant Ca^{2+} buffer and to clamp the intracellular free Ca^{2+} ($[Ca^{2+}]_i$) nearly constant. Most of the Ca^{2+} entering or leaving the cell binds to, or comes from, the dominant buffer, which optically reports how much Ca^{2+} it has bound (Tsien et al., 1982; Tsien and Rink, 1983). A variant of this method is to replace the fluorescent indicator by EGTA, which release two protons per Ca^{2+} bound, plus a pH indicator (Jong et al., 1995). Obviously, methods in which $[Ca^{2+}]_i$ is nearly clamped are more suited to measuring Ca^{2+} fluxes into rather than out of the cytoplasm.

Yet another common need is to measure spatial variations in Ca^{2+} content, particularly to localize compartments of high Ca^{2+} within cells. Several methods are available for microscopic quantitation of total Ca^{2+} within fixed or quick-frozen tissue sections, including laser-activated mass spectrometry and various electron microscopic techniques (Somlyo et al., 1988; Baumann et al., 1991; Wendt-Gallitelli and Isenberg, 1991; Chandra et al., 1994; Grohovaz et al., 1996). Perhaps the most challenging aspect of these methods is the problem of preventing redistribution of Ca^{2+} during sample preparation for electron microscopy.

Free Ca^{2+} Monitoring by Aequorin, Metallochromic Indicators, Ion-Selective Electrodes, and Bioassay

Most Ca^{2+} measurements nowadays focus on the concentration of intracellular free Ca^{2+}, abbreviated as $[Ca^{2+}]_i$. Such measurements require placing a known Ca^{2+} binding sensor inside the cell(s) and measuring the extent to which the sensor becomes Ca^{2+}-occupied. The first practical sensor molecule was a chemiluminescent protein, aequorin, extracted from bioluminescent jellyfish (*Aequorea forskalea* or *victoria*) that live in Puget Sound. Once aequorin binds its full complement of Ca^{2+} ions, three per protein molecule, it emits blue light. The actual emitting chromophore is a small organic cofactor, coelenterazine, which is destroyed in the process. The uses, advantages, and disadvantages of aequorin have been extensively reviewed previously (Campbell et al., 1979; Blinks et al., 1982; Thomas, 1982; Cobbold and Rink, 1987; Cobbold and Lee, 1991; Miller et al., 1994; Rizzuto et al., 1994b). The main disadvantages of aequorin are as follows: (1) it is irreversibly destroyed by high Ca^{2+}; (2) the light output is very low, because on average twelve Ca^{2+} ions have to bind to and consume six aequorin molecules to cause the emission of just one photon (Shimomura, 1995), so that imaging of individual small cells is difficult (Rutter et al., 1996) or impossible; (3) the light output is a steep 2.5th power law with respect

to $[Ca^{2+}]_i$, so that when aequorin is exposed to spatially nonuniform $[Ca^{2+}]_i$, its signal is heavily biased towards the highest local $[Ca^{2+}]_i$ values; (4) it is technically quite difficult to introduce the intact preformed protein into cells without exposing either to high Ca^{2+}, even momentarily. The main new development in the last few years (Rizzuto et al., 1994b) has been the use of the aequorin gene and molecular biological techniques to cause the protein to be synthesized in situ and targeted to specific organelles within cells such as mitochondria (Rizzuto et al., 1994a), nuclei (Brini et al., 1994), and endoplasmic reticulum (Montero et al., 1995; Button and Eidsath, 1996; Kendall et al., 1996). Fortunately, coelenterazine is commercially available, membrane-permeant, and spontaneously able to bind to the apoprotein to form functional aequorin as a Ca^{2+} sensor in the desired location. Aequorin is thus particularly advantageous for assessing free Ca^{2+} levels in specific organelles or sites to which it can be targeted by molecular biological signals. It is also useful in organisms such as bacteria, yeast (Nakajima-Shimada et al., 1991), slime molds (Cubitt et al., 1995a), and plants (Campbell et al., 1996), whose cells are easy to transfect but difficult to load with small-molecule fluorescent indicators, and in subpopulations of cells that are cotransfected with other genes of interest (Brini et al., 1995). Aequorins of reduced Ca^{2+} sensitivity have been engineered to extend the measurement range to higher concentrations (Shimomura et al., 1993). However, Ca^{2+} levels reported by aequorin in the lumen of the endoplasmic reticulum are contentious (Montero et al., 1995; Button and Eidsath, 1996; Kendall et al., 1996), probably because that organelle is heterogeneous and because the high Ca^{2+} not only stimulates light output but also kills the protein.

Nonfluorescent metallochromic dyes such as murexide, arsenazo III, antipyrylazo III used to be very popular indicators of intracellular Ca^{2+} (Tsien and Rink, 1983; Thomas, 1991). The Ca^{2+} changes their absorbance spectra mainly by displacing H^+, which makes their Ca^{2+}-sensitivity intrinsically pH-sensitive. Other problems include low affinity and complicated stoichiometry for Ca^{2+}, low selectivity against Mg^{2+}, the insensitivity and difficulty of calibrating absorbance signals in thin cells, the lack of membrane-permeant ester derivatives, and their tendency to react with NAD(P)H and sulfhydryls to generate free radicals and superoxide (Beeler, 1990; Docampo et al., 1993). Currently, the main area where metallochromic dyes have significant advantages is in the measurement of very fast $[Ca^{2+}]_i$ transients in amphibian skeletal muscle. Modified murexides have Ca^{2+} dissociation constants just below 1 mM, so that they can respond quickly and linearly to $[Ca^{2+}]_i$ elevations of tens of micromolar. Their low molecular weight minimizes binding to cytosolic components-(Hirota et al., 1989).

The two major nonoptical methods for quantifying $[Ca^{2+}]_i$ are Ca^{2+} selective microelectrodes and nuclear magnetic resonance (NMR) of fluorinated indicators. Ca^{2+}-selective microelectrodes (Thomas, 1982; Orchard et al., 1991; Baudet et al., 1994) consist of a glass micropipet plugged with a viscous organic matrix doped with a Ca^{2+}-selective ionophore. Because of the ionophore, the membrane is selectively permeable to Ca^{2+}, so that the potential across the membrane approaches the Nernst potential for Ca^{2+} and changes by about 29 mV per decade change in $[Ca^{2+}]_i$. The unique advantage of Ca^{2+}-selective microelectrodes is their wide dynamic range, from 10^{-8} to $> 10^{-2}$ M$[Ca^{2+}]$, thanks to the inherently logarithmic response. However, they have many difficult aspects. Each microelectrode needs to be individually fabricated and calibrated, which takes considerable skill and effort. The selectivity of the ionophore is not absolute, so the response levels off in the region of 10^{-7} to 10^{-8} M. Response times are small fractions of seconds at high $[Ca^{2+}]$, but slow down to seconds or tens of seconds at typical resting $[Ca^{2+}]_i$. It is hard to make tips below 0.5μm in diameter, which limits impalements to relatively large and sturdy cells. Even when an impalement is achieved, the absolute potential of the electrode then includes the membrane potential across the plasma membrane. The plasma membrane potential needs to be measured with a separate electrode and subtracted. Thus, two simultaneous high-quality membrane impalements are required. Any leak at either electrode can let Ca^{2+} into the cell or depolarize the membrane and thereby distort the results. The $[Ca^{2+}]_i$ measurement comes from a single point inside the cell, which could give valuable spatial resolution if one knew exactly where the tip is relative to other cellular landmarks, but this is often not the case. For all these reasons, intracellular Ca^{2+}-selective microelectrodes are rarely used nowadays.

The NMR indicators are chemical relatives of the fluorescence indicators and will be discussed after the latter.

Because cells have so many Ca^{2+}-sensitive functions, it is sometimes possible to use a relatively well-characterized endogenous response as a nonperturbing internal bioassay for $[Ca^{2+}]_i$. This approach is particularly attractive for monitoring $[Ca^{2+}]_i$ in specific locations that are difficult for exogenous indicators, such as the immediate vicinity of plasma membrane Ca^{2+} channels or secretory vesicles (Chow et al., 1994). The problems lie in independently calibrating the endogenous Ca^{2+} sensor, for example using Ca^{2+} buffers and caged Ca^{2+}, and in ensuring that its Ca^{2+}-sensitivity remains the same during the physiological phenomena under study.

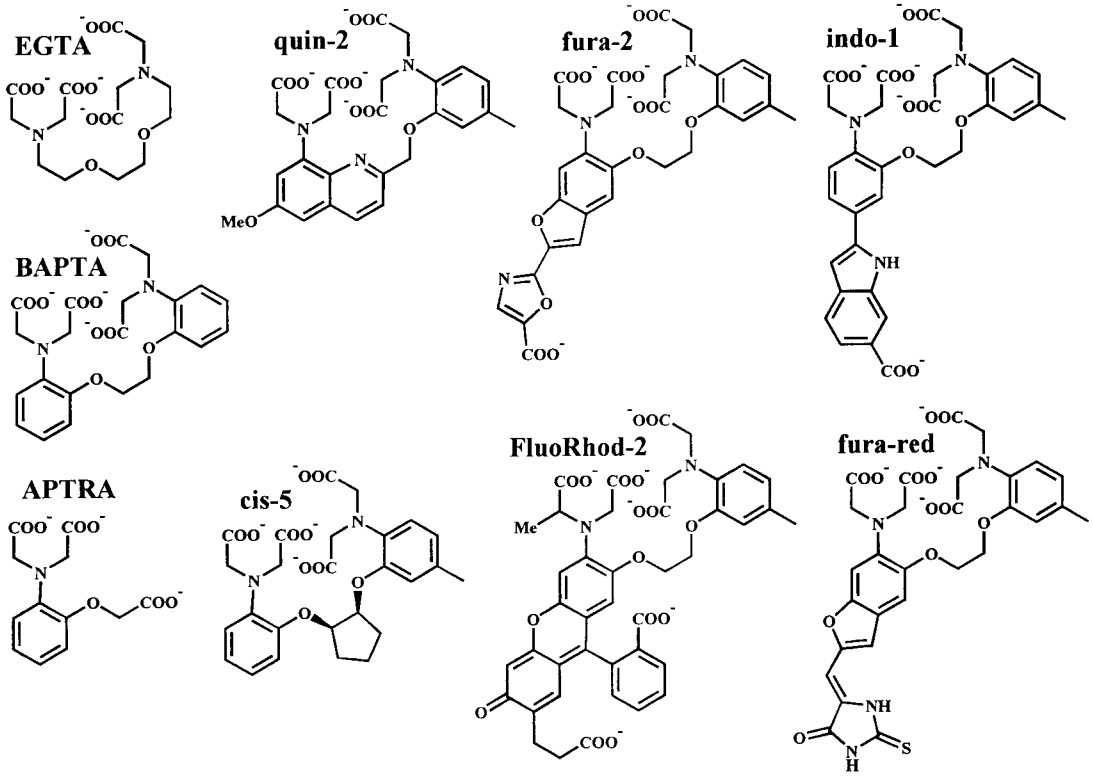

Figure 2.1 Structures of Ca^{2+} chelators EGTA, BAPTA, APTRA, and cis-5, plus fluorescent indicators whose excitation or emission wavelengths are altered by Ca^{2+} binding: quin-2, fura-2, indo-1, FluoRhod-2, and fura-red.

Polycarboxylate Chelators and Indicators for Ca^{2+}

The use of fluorescent polycarboxylate indicators for Ca^{2+} has been reviewed many times (Cobbold and Rink, 1987; Tsien, 1988, 1989a, 1989b, 1992; Tsien and Pozzan, 1989; Williams and Fay, 1990; Callaham and Hepler, 1991; Moreton, 1991; Thomas and Delaville, 1991; Duchen, 1992; Poenie, 1992; Kao, 1994). The current discussion will focus on the general principles and molecular mechanisms rather than catalog the dye properties and biological applications. More practical experimental advice can be found in the above reviews, as well as in the primary literature on the particular tissue or cell type of interest.

BAPTA

Modern Ca^{2+} indicators for biological use are descended from BAPTA (Tsien, 1980), which, in turn, was designed from EGTA (structures in Fig. 2.1), the first chelator shown to have high selectivity for Ca^{2+} over Mg^{2+}. BAPTA has about the same high selectivity ($\sim 10^5$) because it has eight ligand groups in much the same steric arrangement as EGTA. The benzene rings in BAPTA have many beneficial effects. They reduce the proton ionizations (pK_a values) to well below 7, compared with 9.58 and 8.96 for EGTA. Both proton and Ca^{2+} affinities may be further modulated by ring substituents, which do not alter the geometry of the ligand groups. Finally, the aromatic rings constitute primitive chromophores whose absorbance and fluorescence spectra are strongly affected by Ca^{2+}. The Ca^{2+}-sensitive spectra of BAPTA itself are too deep in the ultraviolet to be useful inside cells, though they can be quite useful in checking the concentration and degree of Ca^{2+} saturation of buffer solutions in vitro. The main Ca^{2+} indicators are obtained by elaborating the benzene rings into chromophores and fluorophores with longer wavelengths. Therefore, the

design of indicators and chelators is highly modular; the ligand groups responsible for cation affinity and selectivity interact in a limited but well-defined manner with th chromophore or fluorophore.

APTRA

London, Levy, and colleagues sought to create fluorescent and NMR indicators for Mg^{2+} (Levy et al., 1988; Raju et al., 1989). Because Mg^{2+} is smaller than Ca^{2+} and can accomodate fewer ligands, they truncated BAPTA to reduce its number of chelating groups from eight to five. The result is a chelator called APTRA (Fig. 2.1) for *o*-aminophenol-*N*, *N*, *O*-triacetic acid, whose K_d values for Mg^{2+} and for Ca^{2+} are about 1.45 mM and 18 μM, respectively (S. R. Adams and R. Y. Tsien, unpublished observations). The truncation of the BAPTA binding site has therefore increased the Mg^{2+} affinity by about 1 order of magnitude while weakening the Ca^{2+} affinity by about 2 orders of magnitude. Fluorophores can be attached to APTRA and show spectral responses closely analogous to their BAPTA relatives (Raju et al., 1989). If cytosolic Ca^{2+} remains at values of $< 1\ \mu$M as in resting cells, APTRA-based dyes can indeed be used to measure cytosolic Mg^{2+}, hence their commercial nicknames (Haughland, 1996) "mag-fura," "mag-indo," and "Magnesium Green," etc. Biologists desperate for fluorescent Ca^{2+} indicators of low affinity have seized upon the APTRA dyes to measure micromolar or higher levels of Ca^{2+}, despite their poor selectivity. In this reviewer's opinion, such use of the APTRA dyes should be approached with care; in particular, it is important to get independent confirmation of Mg^{2+} levels or at least determine that they remain constant.

Effect of Substituents on Ca^{2+} Affinities

The simplest way to modify the cation affinities of BAPTA or APTRA in a rational and controllable way is to add electron-donating or -withdrawing substituents, which, strengthen and weaken cation binding, respectively. Chemists have long had parameters that measure how strongly different substituents donate or attract electron density (Perrin et al., 1981). These parameters predict reasonably accurately the effect of the substituents on Ca^{2+} affinities (Tsien, 1980; Pethig et al., 1989). Most of the fluorescent indicators based on BAPTA have a methyl substituent on the benzene ring that lacks the fluorophore. The main purpose for this methyl is to block any further substitution and to ensure that only one fluorophore can be attached to BAPTA, but it also slightly increases the Ca^{2+} affinity. Replacement of this weakly electron-donating methyl by a strongly electron-withdrawing nitro group, as in "Calcium Green-5N" and "Calcium Orange-5N," weakens the affinity by about 70–400 fold (Pethig et al., 1989; Haugland, 1996). A roughly similar weakening results from addition of two fluorine substituents (London et al., 1994).

Another way to modify the cation affinities is to alter the bridge connecting the two halves of BAPTA. Replacement of one of the ether oxygens by an sp^2-hybridized nitrogen, as the quin-1 and quin-2, has relatively little effect on Ca^{2+} affinity but strengthens Mg^{2+} binding by about 5-fold (Tsien, 1980), one of the major disadvantages of quin-2. Inclusion of the central $-CH_2-CH_2-$ group into a five- or six-membered ring greatly constraints its geometry and can either raise or lower the K_d for Ca^{2+} (Adams et al., 1988). Ca^{2+} binding is strengthened by a five-membered ring in which both oxygens sprout from the same side of the ring, i.e., a *cis*-1,2-cyclopentanediyl linkage as in "cis-5" (Fig. 2.1). When the oxygens are attached to opposite sides of the ring, i.e., a *trans*-1,2-cyclopentanediyl linkage, then the K_d is greatly increased. In six-membered (cyclohexanediyl) rings, both stereochemistries tend to weaken Ca^{2+} binding, but by smaller factors. These modification are relatively pure steric effects on the connection geometry between the otherwise unchanged halves of BAPTA, and their respective effects were surprises. They would be good challenges for any theoretical chemist who feels able to predict affinities of cations for ligands in aqueous solution. Nevertheless, the *cis*- and *trans*-1,2-cyclopentanediyl analogs of BAPTA are quite useful, in that the *cis* forms give the highest affinities and Ca^{2+}:Mg^{2+} selectivities of any BAPTA derivatives, and the *trans* forms are useful isomers that provide low-affinity chelators that retain strong rejection of Mg^{2+}.

The remaining locations where substituents have been added are on the chelating arms themselves. Extra methyl groups hanging from the carboxymethyl side arms, as in FluoRhod-2 (fig. 2.1), considerably increase both Ca^{2+} and H^+ affinities. The increase in pK_a brings those values over 7 and therefore makes the chelators pH-sensitive unless electron-withdrawing substituents are also present on the benzene rings, as is the case in FluoRhod-2 (Clarke et al., 1993; Smith et al., 1993). Also, the considerable increase in hydrophobicity will make the dyes difficult to load by means of hydrolyzable esters. Therefore, such dyes have not yet been useful in practical biological measurements.

Effect of Environmental Factors: Ionic Strength, pH and Macromolecules

Aside from molecular substituents, several environmental factors affect Ca^{2+} affinities. Increasing ionic strength weakens Ca^{2+} binding, i.e., raises the K_d as

would be expected for the reaction of a tetra-anion with a divalent cation (Grynkiewicz et al., 1985; Pethig et al., 1989). Temperature per se has relatively modest effects (Lattanzio and Bartschat, 1991), because complexation has only a small enthalpy of reaction. The K_d values for Ca^{2+} are typically 1.6–2.2-fold higher at 37°C in ~ 150 mM ionic strength at 20°C in 100 mM KCl (Grynkiewicz et al., 1985; Merritt et al., 1990), but most of this difference is due to the ionic strength rather than the temperature. Increasing acidity or Mg^{2+} concentrations generally have modest effects on BAPTA-based indicators until pH <6.5 or $[Mg^{2+}] > 10$ mM are attained. Furthermore, even when these competing cations bind, they alter the spectra of most indicators relatively little, because they primarily bind to just the half of the BAPTA that does not carry the fluorophore (Minta et al., 1989; Tsien, 1980). By contrast, Ca^{2+} engages hasboth halves of BAPTA simultaneously and therefore has both a higher affinity and larger spectral effect. Of course, the APTRA-based indicators are much more vulnerable to Mg^{2+} perturbation. Finally, binding to certain macromolecules is reported to weaken the indicator's Ca^{2+} affinities considerably (Konishi et al., 1988; Blatter and Wier, 1990; Bancel et al., 1992; Zhao et al., 1996), especially in skeletal muscle. The seriousness of this problem, in practical biological applications is controversial (Westerblad and Allen, 1994).

Reaction Kinetics

Because the BAPTA nucleus is already fully ionized, Ca^{2+} can bind to an empty BAPTA moiety at essentially diffusion-controlled rates, i.e., rate constants of $10^8 - 10^9\ M^{-1}\,s^{-1}$. The rate constants for dissociation vary in order of magnitude from 10^2 to $10^4\ s^{-1}$ for k_d values of 0.1 to 100 μM (Quast et al., 1984; Kao and Tsien, 1988; Eberhard and Erne, 1991; Lattanzio and Bartschat, 1991). Higher K_d values result mainly from increased dissociation rate constants, with only modest decreases in association rate constants.

Fluorescence Characteristics ad How They are Affected by Ca^{2+} and Other Cations

In order for Ca^{2+} to bind to all the ligand groups simultaneously, the bond between the nitrogen and the aromatic ring has to twist by about 90° so that the lone pair of electrons from the nitrogen can point toward the Ca^{2+} placed symmetrically between the two ether oxygens. This twist, together with the electrostatic attraction of the Ca^{2+} for the electrons, prevents them from conjugating with the rest of the benzene ring or any attached chromophore. Therefore, the effect of Ca^{2+} binding can be generally predicted by conceptually disconnecting the nitrogens from the rest of the molecule. This steric twist was initially predicted by model building (Tsien, 1980) but later confirmed by x-ray crystallography (Gerig et al., 1987). An additional effect of the Ca^{2+} is an overall rigidification of the ligand configuration, which tends to inhibit vibrational deactivation and thereby makes the fluorescence quantum efficiency of the Ca^{2+} complex generally higher than that of the metal-free indicators.

Quin-2

Quin-2 was the first fluorescent tetracarboxylate indicator that was of practical biological use as an intracellular Ca^{2+} indicator. Like most tetracarboxylate indicators from the Tsien lab, its name reflects the first four letters of the name of the fluorophore, followed by a number giving its chronological order within its chemical series. Quin-2 was thus the second completed quinoline derivative of BAPTA (Tsien, 1980). Its structure is shown in Fig. 2.1. The chromophore consists of a 6-methoxyquinoline, whose extinction coefficient and fluorescence wavelengths are rather similar to dansyl groups. The quinoline fluorophore includes a ring nitrogen, which takes the place of one of the ether oxygens of BAPTA. The double function of the quinoline keeps the molecule very compact, but lowers the Ca^{2+}:Mg^{2+} selectivity by almost an order of magnitude. Fortunately, the excitation spectra of the free dye and of the Mg^{2+} complex cross at 337 nm, so, at this wavelength, Mg^{2+} binding happens not to alter the fluorescence, although it is still a silent inhibitor of Ca^{2+} binding. The Ca^{2+} binding causes a larger spectral shift, but the most obvious effect is a 6-fold increase in excitation amplitude a this wavelength, which is the traditional setting for working with quin-2. The usual estimate of 115 nM for the effective K_d for Ca^{2+} at 37°C assumes a free Mg^{2+} of 1 mM (Tsien et al., 1982). Quin-2 is little used nowadays because it has a relatively small extinction coefficient, low quantum yield even when bound to Ca^{2+}, and is relatively photobleachable, all of which make it almost impossible to image microscopically. Other drawbacks include the poor selectivity for Ca^{2+} over Mg^{2+} and other divalent cations and the difficulty of deducing Ca^{2+} from the ratio of the fluorescences obtained at two wavelengths (Grynkiewicz et al. 1985). The lack of ratiometric readout is because the quantum yield of the Ca^{2+} complex is so much greater than the free dye that their spectra do not have a useful crossover point. The main advantage of quin-2 is that because it is the smallest tetracarboxylate indicator that is sufficiently fluorescent to be detected intracellularly, its permeant acetoxymethyl (AM) ester is the most efficient at depositing high concentrations of quin-2

inside cells. Therefore, quin-2 is particularly useful (Tsien et al., 1982; Tsien and Pozzan, 1989) when (1) millimolar or higher concentrations of intracellular chelator need to be attained by the permeant ester technique and (2) those dye concentrations and the efficacy of Ca^{2+} buffering need to be quantified by fluorescence measurements, which are impractical with BAPTA.

Fura-2

Fura-2 (structure in Fig. 2.1) is probably the most popular Ca^{2+} indicator (Grynkiewicz et al., 1985; Tsien, 1989a) because it combines convenient excitation ratioing, fairly good photostability, and relatively easy loading via its acetoxymethyl ester fura-2/AM, which made it the first that could be readily imaged at the single-cell level (Tsien and Poenie, 1986). The name "fura-2" reflects its origin as the second member of a family of indicators containing benzofuran groups. Free fura-2 has an excitation peak at 362 nm, which shifts to 335 nm and increases in amplitude upon binding of Ca^{2+} (Fig. 2.2). The K_d for Ca^{2+} is 135 nM in 100 mM KCl at 20°C, vs. 224 nM in buffer-simulating mammalian cytoplasm at 37°C. The emission peak, at 518 nm for the free dye, shifts only to 510 nm when Ca^{2+} binds (Grynkiewicz et al., 1985), probably because in the excited state the amino group disengages from the Ca^{2+}. The evidence for such excited-state relaxation is that when fura-2 solutions are made highly viscous, for example by addition of 70% sucrose and chilling to −10°C, Ca^{2+} binding then causes about a 55 nm shift to shorter wavelengths (R. Tsien, unpublished observations).

Indo-1

Indo-1 (Fig. 2.1) is unique among the commercially available Ca^{2+} indicators in shifting not only its excitation but also its emission wavelengths (from 482 to 398 nm) upon Ca^{2+} binding (fig. 2.2). The K_d for Ca^{2+} in buffers mimicking mammalian cytoplasm at 37°C is 250 nm (Grynkiewicz et al., 1985). A probable reason for the emission shift is that the indole fluorophore is unusually electron-rich, so that it is less prone than the oxazole of fura-2 to steal electron density from the BAPTA amino nitrogen in the excited state. Therefore, the Ca^{2+} is retained in the binding site and keeps the emission wavelengths short. Emission ratioing is particularly valuable for instruments such as flow cytometers and confocal microscopes that use laser excitation, because it is relatively inconvenient to alternate between two UV excitation lasers at 340 and 380 nm. It is much easier to excite with a single UV laser at 351 or 364 nm and to ratio the two emission bands that are simultaneously produced, especially when a pair of inexpensive photomultipliers or other nonimaging detector can be used instead of imaging cameras. Emission ratioing requires no wavelength-selecting moving parts and is not limited in speed by the rate of alternating excitation wavelengths.

One of the most exciting trends in laser-based microscopy is multiphoton excitation, the use of very brief but high-intensity pulses of focused infrared light to excite dyes that normally require UV photons (Xu et al., 1996). If two or even three IR photons hit the dye molecule essentially simultaneously, which means within a femtosecond or so, their energies may add together to produce the same result as a single photon of twice or treble the energy, i.e. $\frac{1}{2}$ or $\frac{1}{3}$ the wavelength. Once the excited state is reached, the subsequent fluorescence properties are the same regardless of whether the excitation energy had been delivered by single UV or multiple IR photons. The main advantages of multiphoton excitation are that (1) the excitation beam is infrared, which penetrates biological tissue much further and with less attenuation than ultraviolet, and which is less subject to chromatic aberration from microscope optics; (2) the very high instantaneous photon fluxes necessary for the low-energy photons to cooperate are achieved only at the focus point of the laser, not above or below that focus. Therefore, dye molecules in out-of-focus planes are not excited and not subjected to photodegradation, and a confocal aperture is not necessary for depth resolution. By contrast, out-of-focus molecules are being wastefully excited and degraded in ordinary confocal microscopy, even though their emission is filtered out by the confocal pinhole that creates depth resolution. The main disadvantage of multiphoton excitation is the major expense and complexity of infrared lasers with femtosecond pulsewidths. Indo-1 is currently the only dye that permits ratiometric measurements of $[Ca^{2+}]_i$ with multiphoton excitation (Szmacinski et al., 1993). The two-photon excitation spectrum of indo-1 is unfortunately peaked at wavelengths somewhat shorter than twice the ordinary (i.e., one-photon) excitation spectrum; the necessary wavelengths, especially for the Ca^{2+} complex, are at or below 700 nm (Xu and Webb, 1996), which is at the very limits of the tuning range of currently available pulsed lasers. Three-photon excitation may actually be somewhat more convenient (Xu et al., 1996).

Miscellaneous Longer Wavelength, Wavelength-Shifting Indicators

Yet longer wavelengths of excitation and emission are possible while retaining wavelength shifts, though tradeoffs must be accepted. For example, DeMarinis et al. (1990) developed an analog of fura-2 in which

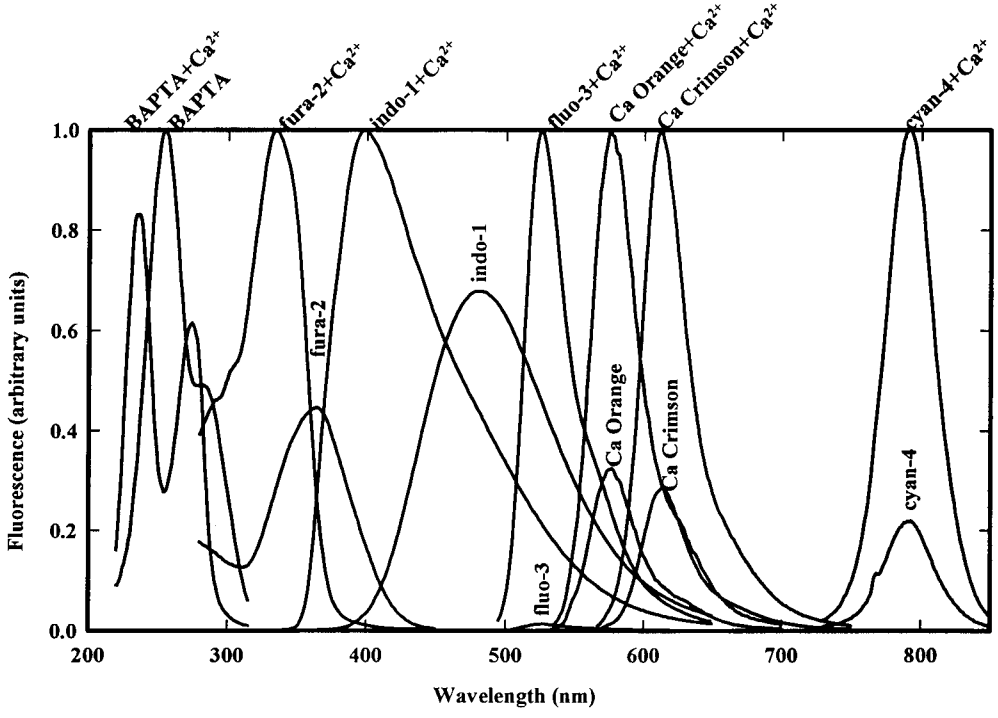

Figure 2.2 Typical fluorescence spectra of Ca^{2+} indicators with and without Ca^{2+} bound, normalized by the maximal amplitude within each pair. Therefore, the relative amplitudes of the free vs. bound forms are shown realistically, but not the relative brightnesses of different indicators. Excitation spectra are shown for BAPTA and fura-2, emission spectra for all the other indicators. Because indo-1 shifts both its excitation and emission wavelengths upon binding Ca^{2+}, the relative amplitudes of the free vs. bound emission spectra depend on excitation wavelength, which was 339 nm for these curves. Data for Ca-Orange and Ca-Crimson courtesy of M. Kuhn and P. Hewitt, Molecular Probes.

the oxazole is replaced by yet longer and more electron-withdrawing groups. The main commercially available example is "fura-red" (Fig. 2.1). Another styryl-based Ca^{2+} indicator without the furan bridge was reported by Akkaya and Lakowicz (1993). Unfortunately, such dyes, which are really styryl merocyanines, tend to have very low quantum yields in aqueous solution. This dimness is probably because the major redistribution of electron density in the excited state from the amino group to the electron-withdrawing end of the chromophore causes a large change in dipole moment, which causes massive redistribution of the surrounding water dipoles, which promotes vibrational deactivation before the excited state can emit a photon. Likewise, several BAPTA-based oxazones and carbazones were developed, but their Ca^{2+} affinities were greatly depressed by the chromophores's strong electron withdrawal, and the quantum yields were disappointing (Tsien, 1983). A later development was FluoRhod-2 (Fig. 2.1), in which the BAPTA is made an integral part of a rhodamine chromophore (Smith et al., 1993). This dye changes from rhodamine-like (excitation and emission maxima at 537 and 566 nm, respectively) to fluorescein-like spectra (480 and 537 nm) upon binding Ca^{2+} with a K_d of 1.07 μM. Unfortunately, no biological results in live cells have been reported yet. Along the same lines, incorporation of BAPTA into a coumarin chromophore generates "BTC," which binds Ca^{2+} with a K_d near 10^{-5} M, while shifting its excitation maximum from 462 to 401 nm (Iatridou et al., 1994). In skeletal muscle, BTC appears to be particularly strongly bound to myoplasmic constituents and to sense some signal other than $[Ca^{2+}]_i$ (Zhao et al., 1996).

Non-Wavelength-Shifting Indicators: General Principles

For many purposes, it is very helpful to be able to excite the indicator fluorescence with visible light. The most common reason is that laser-based

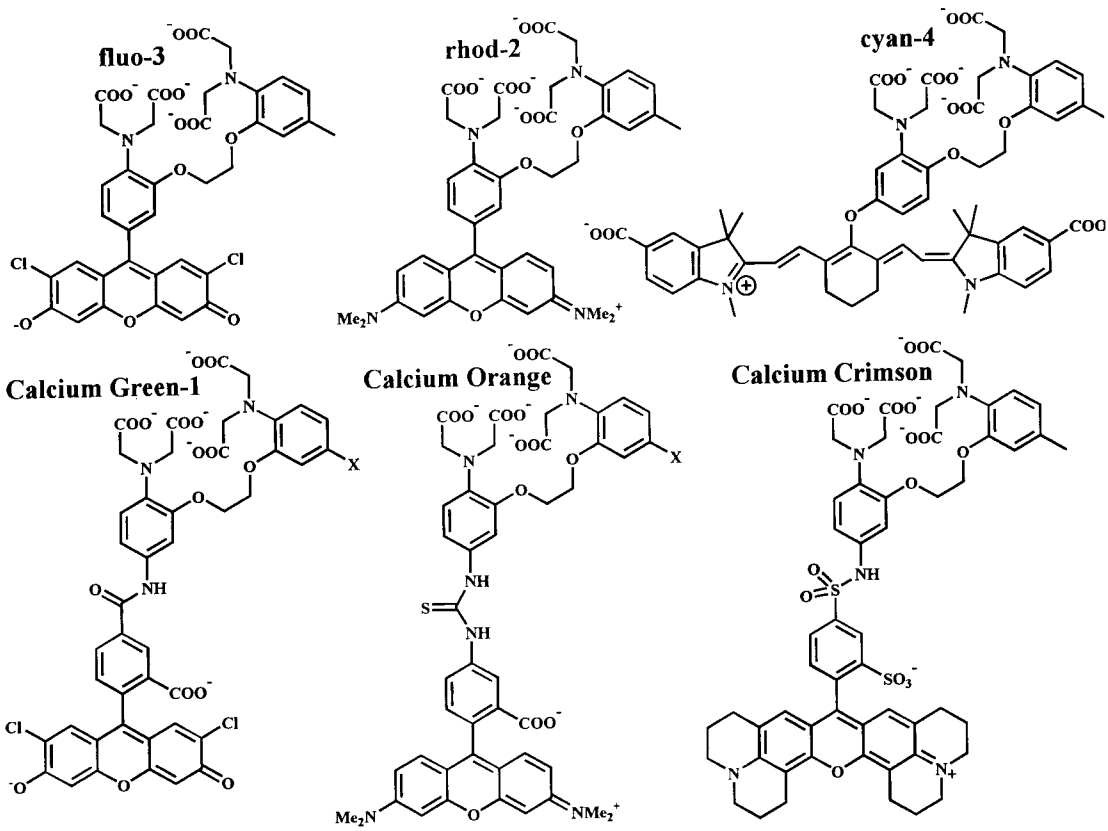

Figure 2.3 Structures of some longer wavelength Ca^{2+} indicators that work by modulation of photoinduced electron transfer: fluo-3, rhod-2, cyan-4, Calcium Green-1, Calcium Orange, and Calcium Crimson.

instruments, such as flow cytometers and confocal microscopes, are often supplied only with visible excitation, most commonly 488 nm from an argon-ion laser. Ultraviolet lasers are certainly available but consume more power, cooling capacity, and initial expense. Sometimes the instrument optics or sample chambers use glasses or plastics that do not pass ultraviolet or that emit fluorescence at those wavelengths. Occasionally, the biological preparation genuinely demands relatively long wavelengths, perhaps because of excessive autofluorescence or light sensitivity at short wavelengths. The most commonly used visible-excitation Ca^{2+} indicators, such as fluo-3, rhod-2, Ca-Green, Ca-Orange, and their analogs (Fig. 2.3), do not shift excitation or emission wavelengths significantly between Ca^{2+}-free and Ca^{2+}-bound forms. Instead, Ca^{2+} binding merely increases the quantum yield and hence the intensity of emission.

All of these dyes contain a fluorophore that is linked to, but clearly distinct from, the BAPTA moiety. The mechanism by which Ca^{2+} occupancy affects the quantum yield of the separate fluorophore is a phenomenon called photoinduced electron transfer (Rettig, 1986; Huston et al., 1988; Bisell et al., 1993; Tsien, 1993). Excitation of the fluorophore involves promotion of an electron from the highest occupied molecular orbital (HOMO) to the lowest unoccupied molecular orbital (LUMO) of the fluorophore. Naturally, this leaves a vacancy in he HOMO. In the absence of Ca^{2+}, the BAPTA portion of the indicator is quite electron-rich and is able to donate an electron to the fluorophore, which fills the vacancy in the HOMO (Fig. 2.4A). Now the originally promoted electron is marooned in the LUMO with no way to emit a photon while returning directly to the orbital from which it came. Therefore, Ca^{2+}-free BAPTA quenches the fluorescence of the attached fluorophore. Eventually, the electron should return to the BAPTA in a relatively slow, radiationless process that restores the ground state, but the net effect is that the excitation energy is dissipated by two

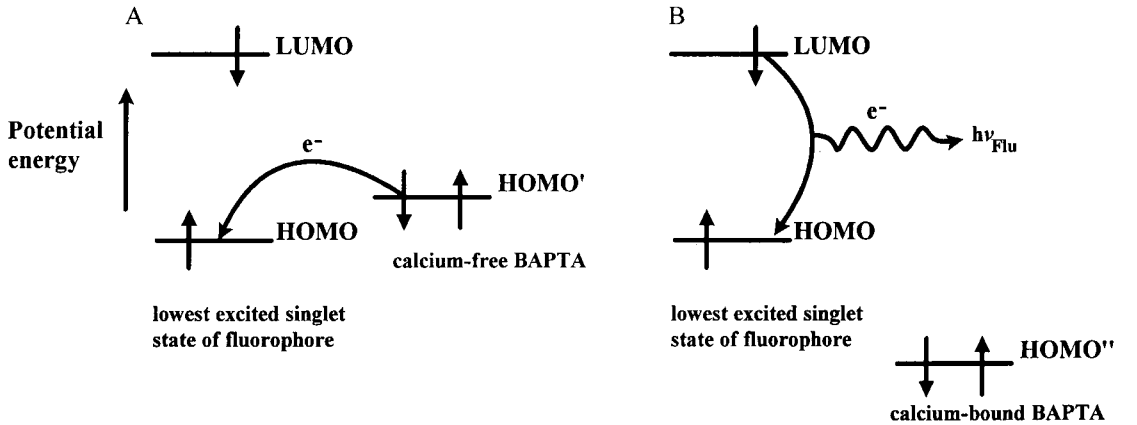

Figure 2.4 Energy level diagrams to explain why nonratiometric visible Ca^{2+} indicators increase their fluorescence upon Ca^{2+} binding. (A) In the absence of Ca^{2+}, the BAPTA unit quenches the attached fluorophore by photoinduced electron transfer. (B) When Ca^{2+} is bound, photoinduced electron transfer becomes energetically unfavorable.

successive electron transfers to and from the fluorophore. By contrast, Ca^{2+}-bound BAPTA cannot donate an electron to the HOMO (Fig. 2.4B) because the Ca^{2+} both electrostatically attracts electron density and decouples the nitrogen lone pair electrons from the rest of the molecule by the steric twist mechanism. Therefore Ca^{2+} inhibits the quenching, i.e., enhances the fluorescence. Photoinduced electron transfer and the consequent quenching are naturally more efficient the more direct and close the linkage between BAPTA and the fluorophore. Therefore, dyes such as fluo-3 and rhod-2, in which the linkage between the fluorophore and the BAPTA is only one bond, show the lowest quantum yields in their Ca^{2+}-free forms and the highest degrees of enhancement (>100-fold) by Ca^{2+} binding (Haugland, 1996). Early estimates (Minta et al., 1989) giving lower enhancement factors were probably artifacts of contamination by Ca^{2+}-insensitive fluorescent impurities contributing to the fluorescence in the absence of Ca^{2+}.

Fluo-3 and Rhod-2

In fluo-3 (Minta et al., 1989), th fluorophore attached to BAPTA is a fluorescein-like xanthene substituted with two chlorine atoms, whose purpose is to shift the pK_a of the fluorophore down to about 5, safely remote from physiological pH. The chloro substituents also place wavelengths of excitation and emission to 506 and 526 nm, slightly longer than those of fluorescein itself. The main spectroscopic effect of Ca^{2+} binding, as stated above, is a ~ 100-fold enhancement in fluorescence amplitude (Fig. 2.2). Fluo-3's K_d for Ca^{2+} is about 400 nm at 20°C in 100 mM KCl (Minta et al., 1989) and 864 nM at 37°C in the ionic strength of mammalian cytosol. These numbers are distinctly higher than those of BAPTA, fura-2, or indo-1, indicating that the xanthene chromophore is somewhat electron-withdrawing. Rhod-2 has a tetramethylrhodamine-like xanthene chromophore, which is positively charged so that rhod-2 has a yet higher K_d for Ca^{2+}, 570 nM (Haugland, 1996). The previous estimate of 1 μM (Minta et al., 1989) was probably perturbed by impurities.

Calcium Green, Calcium Orange, and Calcium Crimson

Michael Kuhn (1993) at Molecular Probes developed a general approach to produce fluorophore-conjugated BAPTAs, in which 5-amino-5′-methyl BAPTA is conjugated to any of a wide variety of amine-reactive fluorescent probes such as 2,7-dichlorofluorescein isothiocyanate, 5-carboxytetramethylrhodamine *N*-hydroxysuccinimidyl ester, and Texas red sulfonyl chloride. These three produce "Calcium Green-1," "Calcium Orange," and "Calcium Crimson," respectively (Haugland, 1996), in which the chromophores are separated from the BAPTA units by an extra benzene ring and an amide, thiourea, or sulfonamide linkage compared with the direct single-bond connections in fluo-3 and rhod-2. The increased spacer length weakens the interaction between the chromophores and the BAPTA, so that Calcium Green-1 and Calcium Orange show higher quantum efficiencies and Ca^{2+} affinities than fluo-3

and rhod-2 (Haugland, 1996). However, the spacers also greatly reduce the degree of fluorescence enhancement due to Ca^{2+} binding, and their extra molecular weight may hinder loading via permeant esters. Although Calcium Green-1 is not ratiometric, it works well with two-photon excitation to detect local $[Ca^{2+}]_i$ elevations (Denk et al., 1995).

Infrared Indicators Based on Cyanine Fluorophores

The approach of tying BAPTA to an independent fluorophore to produce Ca^{2+}-modulated PET appears to be fairly general and has been exploited to produce both shorter wavelength indicators, using fluorophores like anthracene and pyrazoline (Bissell et al., 1993), and very long-wavelength dyes, using heptamethine cyanines (S. R. Adams and R. Y. Tsien, in preparation). The cyanines yield infrared excitation and emission wavelengths (770 and 790 nm, respectively) that should be very valuable for particular biological problems, such as measurement of $[Ca^{2+}]_i$ in photoreceptors or other cells sensitive to UV and visible wavelengths, in highly pigmented or autofluorescent tissues like blood or green plants, or deep inside scattering tissues. Their K_d values are around 280 nM. However, the very large size and hydrophobicity of the heptamethine cyanine chromophore has hindered purification and successful intracellular delivery of the molecules by permeant esters or patch clamp techniques, though pressure injection through sharp microelectrodes works.

Effect of Competing Cations: Mg^{2+}, Sr^{2+}, and Ba^{2+}

The basis for discrimination between Ca^{2+} and Mg^{2+} is built into BAPTA and has already been discussed. Discrimination of Sr^{2+} and Ba^{2+} from Ca^{2+} is more difficult, not only for synthetic chelators but also for biological processes, which explains why Sr^{2+} and Ba^{2+} are often partial to excellent surrogates for Ca^{2+}. Fura-2 binds Sr^{2+} and Ba^{2+} with K_d values of 780 nM and 2.62 μM, respectively at 37°C (Schilling et al., 1989), i.e., Ca^{2+} is preferred by factors of 3.5 and 11.7, respectively. The spectral effect of Sr^{2+} and Ba^{2+} binding is basically similar to that of Ca^{2+} binding, so in order to use fura-2 to measure free $[Sr^{2+}]$ or $[Ba^{2+}]$, $[Ca^{2+}]_i$ needs to be known and preferably kept constant. Explicit tests of the effect of Sr^{2+} and Ba^{2+} on other BAPTA derivatives have not been reported, but one would expect the Ca^{2+}:Sr^{2+} and Ca^{2+}:Ba^{2+} selectivity ratios to be roughly preserved.

Transition metal ions also bind to BAPTA derivatives, but here the binding is usually much stronger than that of Ca^{2+} and the spectral effect more unpredictable. The most extensive data are for fura-2 and fluo-3. Fura-2 is quenched to practically zero quantum yield by Mn^{2+}, Co^{2+}, and Ni^{2+} (Grynkiewicz et al., 1985), whose paramagnetism presumably promotes intersystem crossing from the excited singlet state to the triplet, and, in turn, from the triplet to the singlet ground state. All three ions are commonly used as blockers for Ca^{2+} channels but Mn^{2+} and Co^{2+} may also permeate such channels to some extent (Shibuya and Douglas, 1992). The ability of Mn^{2+} to sneak through Ca^{2+} channels and quench quin-2 and fura-2 is the basis for a popular method for semiquantitative assessment of plasma membrane Ca^{2+} permeability (Hallam and Rink, 1985). The Mn^{2+} is added extracellularly, typically at 0.1–1 mM. The rate of quenching of the fluorescence is an index of plasma membrane permeability to divalent cations. Such quenching can, at least initially, be measured separately from the free $[Ca^{2+}]_i$ measured by ratioing, because the latter should not be affected by losses of fluorescence at both wavelengths. However, the validity of the method assumes that (1) Mn^{2+} is neither stored inside internal organelles nor pumped back out of the cell and (2) incoming Mn^{2+} does not remain free or bind to cellular buffers but binds essentially exclusively to the dye. Assumption (1) is generally accepted; assumption (2) is more problematic. Very little is known about cellular buffering of Mn^{2+} and its competition with Ca^{2+}. Although fura-2 binds Mn^{2+} about 42-fold more tightly than Ca^{2+} (Grynkiewicz et al., 1985), one must be concerned that when $[Ca^{2+}]_i$ is high, some of the fura-2 may remain bound to Ca^{2+} and unquenched.

Binding of Mn^{2+} to fluo-3 does not quench the fluorescence completely (Minta et al., 1989). Presumably, the metal both prevents photoinduced electron transfer (as does Ca^{2+}) and contributes paramagnetic quenching instead, but in fluo-3 the paramagnetic ion is much further away from the fluorophore than it is in fura-2. The net effect is that the fluo-3–Mn^{2+} complex is about one fifth as fluorescent as the Ca^{2+} complex and simulates about 100 nM free $[Ca^{2+}]_i$. This partial quenching is the basis for one of the few methods for calibrating intracellular fluo-3 signals in terms of absolute $[Ca^{2+}]_i$ without lysing the cell. A Ca^{2+} ionophore, such as ionomycin, is used first to elevate $[Ca^{2+}]_i$ to levels that saturate fluo-3, then the external Ca^{2+} is replaced by Mn^{2+}. The fluorescence levels observed when the fluo-3 is Ca^{2+}- and Mn^{2+}-saturated, together, with the K_d of fluo-3 for Ca^{2+}, are enough to determine $[Ca^{2+}]_i$ (Kao et al., 1989; Merritt et al., 1990).

Heavy divalent cations without unpaired electrons, such as Zn^{2+}, Cd^{2+} and Pb^{2+}, also bind fura-2 and fluo-3 quite avidly. The K_d values are in the low

nanomolar range for Zn^{2+} and picomolar for Cd^{2+} and Pb^{2+} (Tsien, 1980; Minta et al., 1989; Jefferson et al., 1990; Tomsig and Suszkiw, 1990; Hinkle et al., 1992). The effects on the spectra are roughly similar to those of Ca^{2+}, usually with somewhat less enhancement of quantum yield. Lanthanides bind with even higher affinity, which results in dissociation rates on the time scale of seconds to minutes.

Fluorescence Lifetimes

Lifetime Ratioing vs. Wavelength Imaging

The excited-state lifetimes of fluorescent indicators are in the low nanosecond range. Generally, the Ca^{2+}-complex has a longer lifetime than the free dye, as would be expected from the higher quantum efficiency of the former. The difference in lifetimes offers an alternative to dual-wavelength ratioing for measuring the percent Ca^{2+}-occupancy of the dye separately from the total amount of dye, pathlength, lamp intensity, or detector efficiency. The dye with the easiest-to-resolve lifetimes is quin-2, which changes from 1.35 to 11.6 ns lifetime upon binding Ca^{2+} (Lakowicz et al., 1992b, 1994). Unfortunately, quin-2, as mentioned previously, is not very bright, photostable, or Ca^{2+}-selective. Fura-2 and indo-1 have rather modest changes in lifetime (Szmacinski et al., 1993; Szmacinski and Lakowicz, 1995) and would be more conveniently quantified using their excitation or emission shifts. Fluo-3 ought to have a huge increase in lifetime to match its >100-fold increase in quantum efficiency upon Ca^{2+} binding, but its excited-state photophysics are rather more complicated. The free dye gives rise to at least two excited-state populations: a species that decays too fast to be measured and another species with a lifetime not so different from the Ca^{2+} complex. The detailed structural or conformational changes responsible for the heterogeneity are not understood. The Calcium-(Green, Orange, Crimson) series would seem to be the most promising for lifetime imaging, given that they contain efficient visible-wavelength chromophores, show significant lifetime changes in response to Ca^{2+}, and cannot be ratioed by dual-wavelength techniques (Lakowicz et al., 1992a; Sanders, 1995). However, the lifetimes observed in intact cells seem rather different from those in vitro, so that interpretation and calibration of intracellular signals has remained difficult.

Two-Photon Excitation

Analysis of excited-state lifetimes requires excitation that is modulated at tens to hundreds of megahertz (MHz) or pulsed with nanosecond or shorter durations. The detector must have comparable frequency bandwidth or time resolution, which is not too difficult for a nonimaging detector but quite challenging for a camera-type system. The expense and commercial nonavailability of such imaging systems have greatly limited the exploration of lifetime detection. In my view, the most promising way to develop lifetime imaging is in conjunction with laser-scanning two-photon excitation, which inherently creates pulses of ~ 0.1 ps duration and 80 MHz repetition rate. The detector can be a nonimaging type because the spatial resolution is supplied by the excitation scanning. The outputs from two phase-sensitive detectors, respectively tuned to report photons emitted immediately (say less than 2 ns) vs. later (2–12 ns) after the pulse, could be ratioed (Sanders, 1995), just as signals at two different wavelengths are ratioed at present.

NMR Indicators

Binding of Ca^{2+} to BAPTA- or APTRA-derived chelators affects not only their optical spectra but also their NMR spectra, as expected from the ability of the cation to attract electron density. To be biologically useful, the chelator must be enriched in an isotope detectable by NMR against a low endogenous background. One approach (Robitaille and Jiang, 1992) has been ^{13}C-enrichment, which affects the ^{1}H spectrum, but a much more popular isotope is ^{19}F, the only natural isotope of fluorine. A variety of fluorinated chelators have been prepared (Metcalfe and Smith, 1991, London et al., 1994). Their major advantage is complete indifference to tissue opacity of autofluorescence, so that $[Ca^{2+}]_i$ can be monitored in brain slices (Badar-Goffer et al., 1990) and intact beating heart (Harding et al., 1993). Disadvantages include the expensive specialized NMR spectrometers required, the need to keep the preparation alive deep inside a superconducting magnet cavity, and the insensitivity of NMR detection. The latter necessitates relatively high concentrations of intracellular chelator ($\sim 100\,\mu M$) and long acquisition times (>10 min), while preventing much spatial resolution. If the tissue undergoes repetitive Ca^{2+} transients that can be synchronized to the NMR pulses, millisecond time resolution can be achieved by stroboscopically varying the time delay (Harding et al., 1993).

Fluorescently Labeled Ca^{2+}-Sensitive Proteins

The two best characterized Ca^{2+}-sensitive proteins, troponin C and calmodulin, have each been labeled by an environmentally sensitive fluorophore, dansylaziridine and a merocyanine, respectively. Their

fluorescence thereby becomes sensitive to the Ca^{2+} occupancy of the protein. Although preparation and microinjection of the labeled proteins are too cumbersome for routine monitoring of cellular Ca^{2+}, these probes can give useful insights into the physiological interactions of these two important Ca^{2+} sensors (Ashley et al., 1991; Hahn et al., 1992).

Targeting of Chelators/Indicators Inside Cells

Microinjection, Iontophoresis, Internal Perfusion, and Electroporation

The most direct techniques for putting the indicators inside cells all involve disruption of the plasma membrane: pressure microinjection, ionthophoresis, internal perfusion with a patch pipet, or electroporation. The first three techniques, which all use micropipets, deliver the dye to one cell at a time, which can be quite helpful in singling out one cell from a complex tissue, but can also be severely restrictive when one would prefer to monitor a larger population at once. Other advantages are that the dye is initially localized solely in the cytoplasm, that its concentration and degree of initial Ca^{2+} loading can often be controlled relatively accurately, and that no chemical modifications or enzymatic activities are required. Major disadvantages are the invasive nature of the procedures and their potential for lasting membrane damage, which would particularly perturb subsequent $[Ca^{2+}]_i$ signals because of the large electrochemical gradient favorig Ca^{2+} entry. Internal perfusion and electroporation cause major replacement of the native intracellular constituents with those supplied by the experimenter, which can cause severe rundown of physiological processes. All the micropipet techniques require considerable skill and specialized equipment.

AM Esters as Membrane-Permeant, Intracellularly Hydrolyzable Derivatives

To avoid disruption of the plasma membrane and the requirement for single cells robust enough for micropipet penetrations, membrane-permeant lipophilic derivatives of the dyes were devised. The idea to mask all the highly polar features, especially the negative charges of the carboxylates, with temporary protecting groups that permit diffusion through the plasma membrane and that fall off inside cell (Tsien, 1981). Similar concepts had been used for delivery of drugs across membrane barriers, but they had, at most, one carboxylate per molecule and delivery into a whole organism was the desired end result (Jansen and Russell, 1965; Ferres, 1980). It was unknown whether molecules with four or more masked carboxylates could cross membranes and whether each individual cell (as opposed to a specialized organ, like the liver) had the capacity to split off the protecting groups intracellularly. Fortunately, AM ester groups proved to confer the desired properties of adequate extracellular stability, membrane permeability, and susceptibility to cytoplasmic esterases. The AM esters are mixed esters of methylene glycol, $CH_2(OH)_2$, in which one hydroxyl is esterified to acetic acid and the other to the carboxylate of the chelator. Sometimes, AM esters have been termed "acetomethoxy," but this name is chemically incorrect. Most of the specificity of intracellular esterases seems to center on the carboxylic acid moeity rather than the alcohol. Simple esters, e.g., methyl or ethyl, or the chelators seem to be poor esterase substrates because the latter is a foreign carboxylic acid. However, acetyl esters are fairly common in biochemistry, so they are readily cleaved by esterases. The free hydroxyl thus released chemically destabilizes the remaining ester, so AM esters are a nice way to transfer the hydrolyzability of acetyl esters onto other carboxylic acid esters. Simple incubation of most mammalian cells with an AM ester results in intracellular accumulation of the parent carboxylic acid over tens of minutes to an hour (Tsien, 1981; Tsien et al., 1982). Because the hydrolysis of the ester groups seems to be due to intracellular esterases, the polyanion reaction products are trapped inside the cells and can accumulate to much higher concentrations than that of the extracellular ester. It must be remembered that all the carboxylates must be hydrolyzed to regenerate the indicator properly. Although the commercially available compounds are the fully anionic and fully esterified forms, intracellular hydrolysis is not an all-or-nothing process but proceeds through an entire set of partially de-esterified intermediates. Even after the initial ester is gone, sufficient time must be allowed for adequate hydrolysis of those intermediates.

The AM esters of BAPTA and quin-2 fairly readily load mammalian cells to final intracellular concentrations of several millimolar. As the indicators were optimized for stronger and longer wavelength fluorescence, the ease of loading generally decreased. Our casual impression, not backed by any quantitative comparisons, is that the loading efficiency with AM esters decreases in the order quin-2 > indo-1 > fura-2 > fluo-3 > Ca Green > cyan-4. This order also happens to fit with increasing molecular weight (except for indo-1 and fura-2, which are almost the same size), so the > 1 kDa moledular weight of the larger AM esters may obstruct permeation through the membrane. Another possibility is that the aqueous solubility of the esters is also decreasing as a steep function of molecular weight. For example, the true

aqueous solubilities of BAPTA/AM and fura-2/AM are 15 and 0.11 μM, respectively (Kao et al., 1990). Therefore, in typical loading protocols using concentrations of fura-2/AM well above the above-quoted solubility, most of the ester is precipitated or bound, and not immediately available to diffuse across the membrane.

The AM esters that have formed precipitates visible under the microscope are probably ineffective at loading cells, but ester that is still colloidal or bound to certain amphiphilic macromolecules still seems able to be transferable to the plasma membrane and from there to reach the cytoplasm. Because its true solubility is so low, it is common practice to disperse the ester as much as possible, for example by gradually squirting the DMSO solution of the ester into a stirred suspension of cells. If the cells are adherent, the DMSO stock solution can be stirred into medium, sonicated briefly, then added to the culture dish.

Ester loading is often improved (Poenie et al., 1986) by including macromolecular amphiphiles such as serum albumin, Pluronic F-127, Cremophor EL, and cyclodextrins, which probably act by reversibly binding the ester, buffering its free concentration, and obstructing precipitation. Albumin is well known to carry hydrophobic molecules in the bloodstream and would be the most physiological of the above adjuvants. Pluoronic F-127 is a block copolymer of propylene oxide and ethylene oxide in which a single macromolecule probably forms a sort of micelle, with the relatively hydrophobic propylene units as the core and the ethylene glycol ethers as the skin. It is a sort of detergent that is relatively nontoxic, perhaps because it cannot split into momoners that make holes in membranes. Two important facts about Pluronic F-127 should be noted. It is not an acid, so the phrase "Pluronic acid" sometimes seen in the biological literature is an oxymoron that has somehow become commonplace through ignorant repetition. "Pluronic" is a tradename from BASF Wyandotte for an entire family of related copolymers. Pluronic F-127 is just one particular member that helps deliver hydrophobic substances like tetrahydrocannabinol and voltage-sensitive dyes to cells (see Lojewska and Loew, 1987, and references therein). It was chosen for trials with AM ester loading merely because it happened to be available in the author's laboratory (Poenie et al., 1986). Other Pluronics might be as good or better. Cremophor EL is another macromolecular detergent, which has been claimed to enable fura-2/AM to load adult brain slices (Kudo et al., 1991). This valuable action has not yet been reproducible in our hands (V. Lev-Ram and R. Tsien, unpublished observations).

Loading of the higher molecular weight indicators via AM esters is often more difficult, or impossible, in microorganisms or plants with cell walls. The AM esters of indicators with big bright fluorophores have molecular masses of 1 kDa or greater, which are probably too high for ready permeation through the cell walls. Also, many of these cell types seem not to have much acetylesterase activity, yet have relatively strong autofluorescence. Even when the dyes are successfully introduced into the cytoplasm, they are often rapidly sequestered into vacuoles (Callaham and Hepler, 1991). For these reasons, successful applications of AM esters in such species are far less common than in vertebrate, especially mammalian, cells.

Alternative Esters

In principle, many derivatives other than AM esters might serve to mask the carboxylates until they get through the membrane. For example, anhydrides or substituted phenyl esters are relatively nonpolar yet hydrolyzable back to the carboxylic acids. Unfortunately, such derivatives are also commonly used to label proteins. Aside from potentially damaging cellular proteins, those dye molecules would be fluorescent but relatively insensitive to Ca^{2+} due to replacement of one or more carboxylates by amides. Alkoxymethyl, silyl, and dialkulaminoethyl esters (Ferres, 1980) spontaneously hydrolyze by different mechanisms that are unlikely to cause labeling of cellular constituents, but have not yet proven effective for getting Ca^{2+} indicators into cells (L. R. Makings, S. R. Adams, and R. Tsien, unpublished observations). *t*-Butyldimethylsilyl esters hydrolyze in 0.5–1 h, a convenient time course, but the partially hydrolyzed intermediates cause lysis of the erythrocytes used as a test system (R. Tsien and V. L. Lew, unpublished observations). A general concern with any substrate that spontaneously and nonenzymatically hydrolyzes quickly enough to load cells is that it will also be sensitive to moisture during storage and will probably have to be prepared freshly before use.

An acetoxymethyl ester is just one of a large family of acyloxyalkyl esters that should all load cells by the same mechanism. Formyloxymethyl would be a very attractive alternative, because it would reduce both the molecular weight and the hydrophobicity, and formyl groups are generally considered more labile than acetyl groups. Unfortunately, formyloxymethyl esters of tetracarboxylate chelators have so far proven difficult or impossible to synthesize (A. Minta and R. Tsien, unpublished observations). Various other esters such as 1-(acetoxy)ethyl, (methoxycarbonyloxy)-methyl, and (methoxyacetoxy)methyl, have been prepared (M. Poenie, S. R. Adams, R. Tsien, unpublished observtions) but none has shown any advantage over AM esters.

A final possibility would be to use photolabile ester groups such as *o*-nitrobenzyls or related caging groups. The ester molecules would be loaded into the tissue in the absence of UV, then photolyzed to trap some of the carboxylates intracellularly. The problems with this approach would be the high molecular weight and hydrophobicity of esters carrying four or five caging groups; the need to photolyze every ester group in order to regenerate full Ca^{2+}-binding affinity; the lack of enzymatically driven intracellular accumulation and the tendency of BAPTA chromophores to quench the photolysis reaction, probably by photoinduced electron transfer (Adams et al., 1989).

Leakage and Compartmentation

The first trials with quin-2/AM loading indicated that the quin-2 was deposited mainly in the cytoplasm and nucleus, as judged by selective permeabilization of the plasma membrane with digitonin or electroporation (Tsien et al., 1982). When fura-2/AM was introduced, microscopic imaging of the dye in single cells became possible. It soon became evident that a significant amount of the dye could be taken up into organelles (Almers and Neher, 1985; Malgaroli et al., 1987; Connor, 1994), especially if the loaded cells were kept at 37°C for long periods. In principle, such compartmentation could occur either by the ester crossing two membranes and becoming hydrolyzed inside the organelles, or by transport of partially or fully anionic dye from the cytoplasm into the organelle. The former possibility might seem more likely, and is probably the dominant mechanism. However, in some cell types, sequestration of fura-2 or fluo-3 into organelles and extrusion across the plasma membrane can be inhibited by drugs such as probenecid and sulfinpyrazone (Di Virgilio et al., 1988; Merritt et al., 1990), which are used clinically to inhibit uric acid transport in the kidney. Unfortunately, probenecid and sulfinpyrazone are sometimes ineffective or have unwanted side effects on cell function. Curiously, one well-defined transporter, the multidrug resistance protein MDR1, seems able to extrude the AM esters but not the free acid forms of the dyes (Homolaya et al., 1993).

Ideally, one would alter the dye structure to reduce its ability to be transported. Vorndran et al. (1995) have made significant progress in this direction by linking a positively charged piperazine to fura-2 on the ring that is not attached to the fluorophore. The resulting "fura-PE3" seems to show much less leakage and compartmentation than fura-2, perhaps because the dye is now a zwitterion and should be less susceptible to nonspecific anion transporters.

The most thoroughgoing way to prevent compartmentation and leakage of the dye is to attach it covalently to a macromolecule such as dextran. Conjugates of fura-2, indo-1, and Calcium Green to dextran (Haugland, 1996) are now commercially available and have proven quite valuable in cases where compartmentation or leakage are particularly severe or in which observations over many hours to days are desired. Of coaurse, such indicators can no longer be loaded as membrane-permeant AM esters and probably are unsuitable for ionrophoresis due to the reduction in charge per unit mass. Therefore, pressure microinjection is typically employed.

Targeting to Particular Intracellular Sites or Organelles

There is widesprad interest in the likelihood that open Ca^{2+} channels in the plasma membrane or endoplasmic reticulum generate steep Ca^{2+} gradients within the first few nanometers to micrometers distance from its mouth. For a review, see Augustine and Neher (1992). The evidence for such gradients at submicroscopic dimensions arises mainly from theoretical modeling and from discrepancies between the amplitude and time course of bulk cytoplasmic $[Ca^{2+}]_i$ signals and the behavior of Ca^{2+}-sensing channels and secretory events (Chow et al., 1994). Several factors contribute to the difficulty in directly observing such local signals. Obviously, their submicroscopic spatial extent and high speed pose tremendous problems in achieving adequate sensitivity and signal-to-noise ratio. The high cooperativity of aequorin's response helps it to detect local transients (Llinás et al., 1992) but also makes quantification trickier. The very high Ca^{2+} amplitudes expected, up to hundreds of micromolar, would locally saturate conventional indicators. High concentrations of diffisuble buffers would themselves tend to blur gradients by raising the effective diffusibility of intracelular Ca^{2+} (Neher, 1986; Nowycky and Pinter, 1993). Dextran conjugation should reduce this problem by lowering the diffusibility of the exogeneous buffering sites. However, the better long-term solution would be to target the Ca^{2+} indicators by biochemical affinity or molecular biological sorting to the appropriate locations, rather than relying entirely on the limited spatial resolution of visible light imaging.

A first attempt at such localization has been the attachment of a 12-carbon tail to a derivative of fura-2 (Vorndran et al., 1995). This tail serves to anchor the indicator to membranes such as liposomes, organelles, or plasma membranes. A hydrophilic spacer in the form of a piperazine amide seems necessary between the dodecyl tail and the rest of the dye so

that the latter is not pulled too deep into the membrane. Unfortunately, AM ester loading appears poorly effective, so that the free acid has to be microinjected. Preliminary reports indicate that some selectivity for near-plasma-membrane Ca^{2+} may be obtainable.

Delocalized Positive Charge for Mitochondrial Uptake

Mitochondria can be loaded with Ca^{2+} indicators by two strategies. The first relies on the organelles' large negative membrane potential, which strongly accumulates delocalized cations such as the permeant AM ester of rhod-2 (Minta et al., 1989; Tsien and Bacskai, 1995). As the four esters hydrolyze and the Ca^{2+}-binding site is unmasked, the net charge shifts from +1 to −3, but by then the dye should no nonger be membrane-permeant. Not all the dye winds up in the mitochondria, presumably because some hydrolysis may occur in the cytoplasm before the esters reach the mitochondria, but the usual appearance is of bright dots or worms, readily distinguished from the dimmer diffuse background of cytoplasmic fluorescence. The identity of the organelles is demonstrated by the costaining with mitochondrial markers and the ability of mitochondrial uncouplers to release the Ca^{2+}. An alternative strategy is to reduce the rhod-2 ester to a colorless nonfluorescent dihydro derivative (Hajnóczky et al., 1995). Mitochondria and peroxisomes, perhaps because they specialize in mediating redox processes, accelerate the reoxidation back to the fluorescent dye. Unfortunately, the dihydro derivative also reoxidizes spontaneously and has to be made just before use (Haugland, 1996); also, it is uncharged and cannot itself be accumulated in a potential-dependent manner. For those seriously wishing to image mitochondrial Ca^{2+}, both methods should probably be tried.

Targeting to Particular Neurons

The use of fluorescent Ca^{2+} indicators in intact neural circuits poses special opportunities and problems. The ubiquity of Ca^{2+} channels as the main transducers that mediate biochemical responses to depolarization means that $[Ca^{2+}]_i$ transients are common markers of neuron activity. Under favorable circumstances, the optical signals that result from such $[Ca^{2+}]_i$ transients are much larger than those obtainable from current voltage-sensitive indicators. Therefore, $[Ca^{2+}]_i$ imaging is valuable not just to analyze the biophysics and biochemistry of an important messenger but also as a technique to eavesdrop on ensemble coding in neural networks. However, a major problem has been that adult central nervous system (CNS) tissue tends to load poorly or not at all with the conventional AM esters (Yuste and Katz, 1991). The probable cause is that the esters cannot penetrate the highly tortuous and compacted extracellular spaces in the mature vertebrate CNS. Those cells that do load are usually on the surface of the brain slice, where physiological recording is suspect because of the high percentage of damaged cells. Probably, there is no fundamental defect in membrane permeability or intracellular esterase activity, because healthy neurons in immature slices or dissociated cultures load satisfactorily. Unfortunately, the neuronal connectivity and signal processing in such preparations are different from intact adult brain. Furthermore, even if all the neurons in a mature slice could be loaded, it would often be quite difficult to distinguish individual cells due to their close packing.

Remote loading of AM esters (Regehr and Tank, 1991; Wu and Saggau, 1994; Backsai et al., 1995) or dextran conjugates (McClellan et al., 1994) provides at least a partial solution to these challenges when the neurons of interest extend processes to some remote location. A high concentration of AM ester or dye dextran conjugage is adminisered at that remote site. If necessary, membranes are locally disrupted to promote loading of the free acid or conjugate. Over the next few hours to days, the indicator gradually diffuses or is transported to the imaging zone, where the only neurons that show up are those whose processes pass through the loading zone. The loading site contains much extraneous fluorescence and may be damaged, so the major requirement is that the indicator should spread further and faster than the injury that enabled it to gain entry to the cells.

Chemical and Biological Problems

Like all complex techniques, the use of Ca^{2+} indicators is subject to a number of pitfalls. Some of the more common ones are discussed below, starting with the most chemical problems and ending with the biological concerns.

Chemical Purity and Stability of Nonesterified Chelators

Almost all biological users buy the chelator free acids, esters, or conjugates from a commercial source and are therefore insulated from the nontrivial problems of multistep organic syntheses and quality control. But when such reagents fail to work or seem to have undesirable Ca^{2+}-binding, pharmacological, or fluorescence properties, it is always possible that impurities are at fault (Zucker, 1992) rather than the molecule whose name is on the label. Sometimes, these problems are obvious because

material from different batches or different vendors behaves differently. But often, such comparisons are not available or the impurity is a reproducible artifact, so biological customers must be aware that purity not only should but actually can be checked when problems arise.

BAPTA-family Ca^{2+} chelators are highly polar molecules that generally do not crystallize well, especially as salts. The salts typically contain varying amounts of water and inorganic salts left over from the reagents used to hydrolyze the esters. Such nonfluorescent impurities may not affect the final use of the chelators in solution but mean that the total weight may not yield an accurate estimate of moles of chelator content. The free acids are less likely to contain much inorganic salts, but unfortunately have some tendency to decarboxylate. This reaction converts $-CH_2COOH$ groups to CH_3 groups plus CO_2, which is lost. Such decarboxylation does not greatly affect the spectra but does reduce the affinity for Ca^{2+} significantly. The form of the dye that is most stable and easily purified is usually the ester (e.g., methyl, ethyl, or *t*-butyl, not AM ester) from which the free acid is first prepared. Quantitative hydrolysis of a known weight of such a pure ester is usually the best way to prepare a chelator or indicator solution of known molarity, from which the extinction coefficient of the dye can be measured at a suitable absorbance maximum. Once that value is published, subsequent solutions can be assayed by absorption spectrophotometry. Absolute chelator concentrations are most important when trying to make solutions of defined percent Ca^{2+}-saturation, either to buffer Ca^{2+} or to measure the K_d of the equilibrium. A useful alternative to knowing the absolute concentrations of chelator and Ca^{2+} is to divide the chelator stock solution into two aliquots, carefully titrate one aliquot to Ca^{2+} saturation as detected by no further change in the spectral properties, then mix the nontitrated aliquot with the Ca^{2+}-saturated stock solution in the desired proportions.

Deterioration of fura-2 salts upon standing in solution at room temperature is particularly easy to notice because addition of excess Ca^{2+} no longer produces a high ratio of 340 nm to 380 nm excitation amplitudes. Really fresh fura-2, saturated with Ca^{2+} and measured on a spectrofluorometer with narrow excitation bandwidths, can give a ratio as high as 35 (Grynkiewicz et al., 1985), but this easily declines to < 20 upon careless storage. The loss of ratio is mainly because Ca^{2+} no longer suppresses the 380 nm excitation as effectively as on a fresh sample. The chemical basis for this deterioration has not been determined.

A somewhat distinct problem is the detection of impurities that are spectroscopically similar to the indicator itself. These include incompletely hydrolyzed esters, decarboxylation and certain photodecomposition products, leftover impurities from the synthesis, etc. Unlike water, excess salts, and buffers, such contaminants are detectable by high-performance liquid chromatography (HPLC) or capillary electrophoresis. The main caution is that HPLC in stainless steel equipment is problematical because the chelators tend to leach variable amounts of heavy metals from the steel, which leads to broad peaks and irreproducible retention times. In our lab, we use nonmetallic, "biocompatible" HPLC equipment or fused silica electrophoresis capillaries. Typical HPLC conditions are on octadecyl reverse-phase silica, pH 5–7, a few millimolar EGTA, with methanol/water or acetonitrile/water gradients. Capillary electrophoresis works in capillaries of 50 cm length, 50–75 μm bore, filled with 50 mM borate, pH 8.5, or 10 mM phosphate buffer and electrophoresed at 20 kV (S. R. Adams, unpublished observations).

AM Ester Problems

The membrane-permeant acetoxymethyl esters can also have significant impurities, which, in the worst case, can actually prevent the detection of real biological signals in ester-loaded cells. Because only the contaminants with chromophores matter, AM ester purity can be checked by thin-layer chromatography on silica gel or by reverse-phase HPLC. Reverse-phase HPLC has the advantage that it is more tolerant of DMSO, which is the most common solvent for stock solutions of AM esters. Heavy metal leaching from stainless steel HPLC apparatus is not important because the AM esters have negligible chelating power until hydrolyzed. Even partial hydrolysis makes the compounds very much more polar, i.e., slower-migrating on normal-phase silica or faster-migrating on reverse-phase columns. It is also worth mentioning that partial hydrolysis is unlikely if the AM ester has been reasonably freshly prepared in dry DMSO, which should be exposed to atmospheric moisture as little as possible. Moisture in the DMSO is most readily noticed by checking the melting point as the stock solution comes out of the freezer. Dry DMSO melts at about 18°C, i.e., only just below normal room temperature. A solution that remains liquid at 0–4°C probably contains substantial amounts of water and may begin to hydrolyze the AM ester groups over a few days.

Yet another problem is how to determine whether the AM esters have fully hydrolyzed within the tissue. This should be checked if the apparent $[Ca^{2+}]_i$ signals are much smaller than expected. With some of the dyes, the excitation spectra change somewhat during the hydrolysis process, but seeing some spectral alteration is not a reliable proof that the hydrolysis has proceeded to completion. The most rigorous test

is to do HPLC or capillary electrophoresis on a tissue lysate (Kawanishi et al., 1989; Tran et al., 1995), but often the quantity of material is insufficient or the apparatus may not be available in a physiological laboratory. The next best measure is to use EGTA buffers to titrate a tissue lysate over a range of free Ca^{2+} concentrations near the reported K_d for the fully hydrolyzed dye. If a Scatchard or other binding plot shows a single binding component with the right K_d, then the indicator must be substantially satisfactory (Kao et al., 1989). But if there is a significant component with a much weaker Ca^{2+} affinity, then incomplete hydrolysis should be suspected.

One of the most notorious problems with AM ester loading of cells is that not all the indicator molecules end up in the cytosol or nucleus. A significant fraction can become loaded into intracellular organelles, such as endoplasmic reticulum or mitochondria, where they obviously encounter a different ambient free Ca^{2+}. For most applications, such compartmentation is undesirable. It is minimized by avoiding ester loading altogether, for example by microinjecting or internally perfusing the indicator as a salt or a dextran conjugate. If ester loading is necessary, for example because large populations of cells are to be examined or the cells are too small to tolerate membrane puncture, then compartmentation is generally reduced by exposing cells to the ester for relatively short times and using them fairly quickly without prolonged periods of incubation at higher temperatures, such as 37°C. In some but not all cell types, compartmentation, as well as active extrusion from the cytoplasm, can be reduced by treatment with clinically useful inhibitors of anion transport, such as probenecid or sulfinpyrazone. Also, the zwitterionic indicators, such as Fura-PE3, are supposed to suffer less from compartmentation and extrusion. Compartmentation can often be recognized simply by the blotchy or punctate distribution of fluorescence. A more quantitative criterion is to permeabilize the plasma membrane with saponin, digitonin, or a patch pipet in whole-cell configuration. The truly cytosolic dye should diffuse away rapidly; the remainder, assuming the membrane-delimited organelles remain intact, represents the compartmentalized fraction. For an interesting analysis of compartmentalization, see Connor (1994).

There is considerable interest in measuring Ca^{2+} levels in the Ca^{2+}-accumulating organelles. In this case, the fraction of dye that enters the organelles is to be maximized. A lower-affinity indicator should be used, and prolonged incubation at 37°C may encourage active transport into the organelles (Hofer and Machen, 1993; Short et al. 1993; Hofer and Schulz, 1996). Cytoplasmic dye can be removed by permeabilization or patch pipet dialysis, or it can be simply quenched by dialysis with Mn^{2+}-containing intracellular solutions (Tse and Hille, 1994) as long as one is sure than Mn^{2+} does not alter the Ca^{2+} transport processes of the organelles.

Bleaching and Formation of Fluorescent Ca^{2+}-Insensitive Degradation Products

All fluorescent dyes bleach at some nonzero rate under intense illumination. Obviously, illumination should be curtailed to the minimum necessary to do the experiment. Certainly, the excitation source should be shuttered off whenever one is not collecting data from the specimen. A ratiometric dye provides an additional level of protection from simple bleaching upon illumination, whose effect is simply to lower the amount of fluorophore remaining, without affecting the ratio of the two wavelengths or decay time components. Of course, the signal-to-noise will gradually degrade, but at least the apparent $[Ca^{2+}]_i$ should not be affected by the bleaching. Unfortunately, it has gradually become clear that the main ratiometric dyes to some extent under photodegradation give products that are still fluorescent but have reduced Ca^{2+} responsivity and affinity. This problem was most fully analyzed in the case of indo-1 (Scheenen et al., 1996). When indo-1-loaded cells are subjected to bright excitation, not only does the dye bleach gradually, but also the apparent resting $[Ca^{2+}]_i$ value and amplitude of $[Ca^{2+}]_i$ transients calculated from the emission ratio decrease. Thus, conversion to a fluorescent but relatively Ca^{2+}-insensitive photoproduct competes with overall bleaching. Overall bleaching requires the presence of O_2 but is relatively independent of Ca^{2+} levels. Conversion to the fluorescent, Ca^{2+}-insensitive product does not require O_2 but is inhibited by high Ca^{2+}. Mass spectroscopic analysis shows that the fluorescent, Ca^{2+}-insensitive product results from loss of a $-CH_2COO^-$ chelating arm from indo-1. Fortunately, this photodealkylation can be substantially inhibited by a few micromolar Trolox, which is a commercially available, water-soluble analog of vitamin E. Although this mechanism has been studied in greatest detail with indo-1, a similar phenomenon also occurs, to some extent, with fura-2 (Becker and Fay, 1987) and with Ca-Green (Scheenen et al., 1996). Because Ca-Green is nonratiometric, the loss of Ca^{2+}-sensitivity superficially resembles simple bleaching, which also occurs. The difference is that simple bleaching does not alter the ability of the remaining fluorescence to respond to a Ca^{2+} increase, whereas formation of a Ca^{2+}-insensitive product means that a bigger $[Ca^{2+}]_i$ increase is required to increase the remaining fluorescence by a given percentage. It has not yet been demonstrated whether Trolox inhibits formation of fluorescent Ca^{2+}-insensitive products from fura-2 and Ca-Green.

Calibration

Calibration of intracellular Ca^{2+} indicators requires observation of their readouts (fluorescence intensity, ratio of intensities at two excitation or two emission wavelengths, or excited-state lifetime) at several defined free Ca^{2+} concentrations, under conditions mimicking the normal intracellular milieu as closely as possible. The ideal would be to clamp the $[Ca^{2+}]_i$ in situ at the end of every experiment, but currently available Ca^{2+} ionophores, such as A23187 or ionomycin, do not mediate enough Ca^{2+} flux to guarantee equality of submicromolar Ca^{2+} concentrations across the plasma membrane except when cell ATP has been depleted (Lew et al., 1982; Chused et al., 1987). Permeabilization of the plasma membrane does equalize $[Ca^{2+}]$ but usually releases the indicator as well. A really powerful Ca^{2+}-specific ionophore or insertable channel would greatly aid calibration.

Single-wavelength fluorescence signals F are calibrated in terms of $[Ca^{2+}]_i$ by the equation (Tsien and Pozzan, 1989)

$$[Ca^{2+}]_i = K_d\left(\frac{F - F_{min}}{F_{max} - F}\right)$$

where F_{min} and F_{max} are the respective fluorescences observed at saturating and zero Ca^{2+} and the same concentration of indicator, optical pathlength, source brightness, and overall detector sensitivity. These four parameters are usually so variable that each experiment must be individually calibrated at its conclusion. Autofluorescence cancels out as long as it is a constant. However, any leaked dye contaminates F and should be removed by washing the cells or quenched by extracellular Mn^{2+} or other paramagnetic ion. In a cell suspension in a cuvette, lysis of the cells does not change the macroscopic average dye concentration or pathlength, so permeabilization is usable as a way of clamping $[Ca^{2+}]$ very high and very low. In cells under a microscope or in a flow cytometer, diffusion of already leaked dye into the bathing solution usually keeps its fluorescence contribution down, but the calibration procedure must not let any additional dye out of the microscopic zone of observation.

The great advantage of ratios R of fluorescences at two wavelengths λ_1 and λ_2, $R = F(\lambda_1)/F(\lambda_2)$, is that they cancel out changes in the concentration, pathlength, and instrumental sensitivity, assuming that background autofluorescence has been properly subtracted and that the molecules are not optically shielding one another. Obviously, the dye's spectral properties and Ca^{2+} affinity and the instrument's spectral bias for λ_1 vs. λ_2 will still affect the ratios, but these factors are much easier to keep constant. The calibration equation then becomes (Grynkiewicz et al., 1985)

$$[Ca^{2+}]_i = K_d\left(\frac{R - R_{min}}{R_{max} - R}\right)\left(\frac{S_{f2}}{S_{b2}}\right)$$

where R_{min} and R_{max} are the respective ratios at zero and saturating Ca^{2+}. The new factor of (S_{f2}/S_{b2}), sometimes abbreviated to β, is the intrinsic ratio of intensities of free vs. Ca^{2+}-bound indicator observed at λ_2. The main residual problem is that dyes inside cells behave somewhat differently from dyes in buffers, whose $[Ca^{2+}]$ is easily controlled. Much of the effect can be traced to viscosity-induced alterations in R_{min}, R_{max}, and β, which, in turn, can be minimized by judicious choice of wavelengths (Busa, 1992). However, the possibility of more fundamental protein-induced perturbations, including alterations in K_d, should not be forgotten (see "Effect of Environmental Factors: Ionic Strength, pH, and Macromolecules" above).

Reports of Toxicity

Toxicity refers to biological effects that are not explained by the obvious ability of the chelators to bind and buffer Ca^{2+} and other metal ions such as Zn^{2+}. Because Zn^{2+} is important for many proteins, such as protein kinase C and zinc fingers, the strong (approximately nanomolar K_d) Zn^{2+} affinity of BAPTA-series chelators should not be forgotten. A relatively simple control (Arslan et al., 1985) is to test TPEN, which stands for *N,N'*-tetrakis(2-pyridylmethyl)ethylenediamine, a commercially available chelator with extremely high affinity for Zn^{2+} ($K_d = 10^{-15.6}$ M) and other transition metals (Anderegg et al., 1977), but negligible affinity for Ca^{2+} ($K_d \sim 40\,\mu M$) and Mg^{2+} ($K_d \sim 20$ mM) (Arslan et al., 1985). Because TPEN is membrane-permeant, 20–100 μM extracellular concentration is generally sufficient. If TPEN mimics the effect of the Ca^{2+} chelator, heavy metal chelation should be suspected. If TPEN has no or a different effect, then heavy metal involvement is unlikely. Likewise, TPEN easily strips any heavy metal away from a Ca^{2+} indicator and reveals whether the latter was being perturbed by heavy metals. One recently discovered complication is that TPEN can buffer Ca^{2+} inside internal stores and thereby activate capacitative Ca^{2+} entry (Hofer et al., 1998).

There was an early report that quin-2 loading could alter lymphocyte mitogenic activity (Hesketh et al., 1983), but no comparable complaints about indo-1 and fura-2 have appeared, despite extensive use in many laboratories. The inositol-1,4,5-trisphosphate receptor may be inhibited by high concentrations of BAPTA, though estimates of the severity of

the effect vary (Combettes et al., 1994; Bootman et al., 1995; Patel and Taylor, 1995; Scheenen et al., 1996). This receptor is also subject to strong feedback (both positive and negative) from the Ca^{2+} that it releases, so it is hard to be sure which effects are toxicity vs. very efficient buffering of the submicroscopic local Ca^{2+} (Horne and Meyer, 1995). Nevertheless, direct pharmacological effects of BAPTA are a general concern with the common practice of using very high concentrations of BAPTA to check for local gradients of Ca^{2+}. Obviously, such experiments require stringently high purity of the BAPTA.

The hydrolysis of each AM ester group releases one molecule each of formaldehyde and acetic acid, and one additional proton from the ionization of the chelator free acid. Up to five AM esters need to hydrolyze per indicator molecule loaded. Both the formaldehyde and the acidity (Spray et al., 1984) are potential sources of toxicity. Fortunately, the formaldehyde is gradually generated at low concentrations far below those that fix tissue and not so different from those produced endogenously from demethylation reactions. Also, one can give effective antidotes, such as ascorbate and pyruvate, typically included in the extracellular medium at millimolar concentrations. Ascorbate may work by reversing the reaction of formaldehyde with lysines (Trezl et al., 1983); pyruvate may fuel oxidative phosphorylation and counteract formaldehyde's tendency to inhibit glycolysis (Garcia-Sancho, 1984). These antidotes have even been able to protect the retina (Ratto et al., 1988), which is probably the tissue most sensitive to formaldehyde. As for the acidity, the pH drop (if any) can be measured by various methods, such as the pH indicator BCECF. Once measured, the acidification can be mimicked by extracellular application of appropriate concentrations of permeant acids, such as acetic or propionic acids. The pH can also be clamped by mixtures of weak bases and acids. Finally, useful control compounds for both the formaldehyde and acidification are methylene diacetate and anis-1/AM (Tsien and Rink, 1983), which are AM esters that release the same byproducts but do not generate Ca^{2+} chelators. Methylene diacetate is available from Aldrich Chemical Co.; anis-1/AM, which represents an isolated half of BAPTA, was formerly available from Molecular Probes as N-(o-methoxyphenyl)iminodiacetic acid, AM.

Despite these concerns about BAPTA and AM ester loading, there is some surprising evidence that BAPTA/AM, far from being toxic to whole animals, is actually protective against neuronal ischemia (Tymianski et al., 1993). The mechanism appears not to be brute force buffering of Ca^{2+} elevations but rather diffusional dissipation of $[Ca^{2+}]_i$ microdomains and damping of glutamate release (Tymianski et al., 1994).

Measuring Free $[Ca^{2+}]_i$ vs. Buffering

The Ca^{2+} indicators must inevitably buffer and perturb Ca^{2+} to some extent in the process of measuring it. To detect changes in $[Ca^{2+}]_i$ with as little perturbation as possible, the most important consideration is to use the lowest concentration of indicator that gives an adequate optical signal-to-noise ratio. This requires that the binding vs. unbinding of Ca^{2+} should make the largest possible change in the fluorescence per molecule of indicator. If absolute levels of $[Ca^{2+}]_i$ are to be measured, they should be comparable to the K_d, because it is at the K_d that the fractions of Ca^{2+}-bound and Ca^{2+}-free dye are jointly most sensitive to Ca^{2+}. If a range of $[Ca^{2+}]_i$ levels, from basal to the peak of a transient, are to be accurately quantified, the mathematically ideal K_d is the geometric mean of the extreme concentrations.

The inevitable buffering has three types of possible consequences: depression of basal Ca^{2+}, blunting of transient increases, and blurring of spatial gradients. Depression of basal $[Ca^{2+}]_i$ by AM-ester loaded chelators or indicators is hardly ever significant in cells exposed to normal extracellular Ca^{2+} concentrations. Low $[Ca^{2+}]_i$ is self-correcting because it increases Ca^{2+} influx via capacitative Ca^{2+} entry and starves Ca^{2+} efflux mechanisms. Only if a cell is heavily loaded with Ca^{2+} buffers in the absence of extracellular Ca^{2+}, or if it is continuously perfused with low-Ca^{2+} buffers, is it possible to lower basal $[Ca^{2+}]_i$ to a significant and sustained manner. For example, when several millimolar quin-2 was loaded into cells in zero external Ca^{2+}, the $[Ca^{2+}]_i$ could be lowered to 10–20 nM. However, on restoration of normal external Ca^{2+}, the $[Ca^{2+}]_i$ rapidly rose back to a normal resting value (Tsien et al., 1982). Although the mechanism for the fast $[Ca^{2+}]_i$ restoration was unknown at the time, in retrospect this must have been one of the first manifestations of capacitative Ca^{2+} influx.

The $[Ca^{2+}]_i$ transients are obviously more severely buffered the higher the total concentration of chelator, the closer the $[Ca^{2+}]_i$ to the K_d, and the briefer the Ca^{2+} fluxes. Because the free and Ca^{2+}-bound chelators are more mobile than Ca^{2+} bound to endogenous buffers, the chelators also considerably raise the effective diffusibility of the Ca^{2+} and smooth out spatial gradients of $[Ca^{2+}]_i$. Such effects have been the subject of considerable theoretical and some experimental investigation.

Buffering of $[Ca^{2+}]_i$ is highly desirable for many types of experiments, for example to determine the biological function of $[Ca^{2+}]_i$ transients or gradients. If these spatiotemporal fluctuations are necessary for

a cell function, introduction of enough chelator should prevent the relevant physiology. Even if the $[Ca^{2+}]_i$ transient is too brief or microscopically localized to be directly monitored, an indirect idea of its magnitude can often be obtained by trying chelators of varying K_d values and seeing which are the most effective, e.g. (Speksnijder et al., 1989; Ranganathan et al., 1994). If some or all of the chelator is a fluorescent indicator, its signal helps to determine the concentration of chelator and the extent to which $[Ca^{2+}]_i$ has been stabilized. Often, $[Ca^{2+}]_i$ is crucially involved in complex feedback loops; inclusion of sufficient buffering power serves as a sort of $[Ca^{2+}]_i$ clamp that can help disentangle the individual reactions, just as voltage clamping separates ionic permeabilities. Finally, once the exogenous chelator becomes the dominant intracellular buffer, changes in its Ca^{2+}-loading become measures of Ca^{2+} fluxes. Often, it is desirable to vary the concentration or K_d and to extrapolate to infinite chelator concentration (Tsien and Rink, 1983). A particularly useful application has been to measure the fraction of an ionic current that is carried by Ca^{2+}; the total charge (integral of the current) is compared with the Ca^{2+} flux measured by the fluorescent indicator under conditions where it buffers the $[Ca^{2+}]_i$ well enough to shield endogenous buffers (Schneggenburger et al., 1993).

Prospects for the Future

What are the most likely areas for major future progress in the monitoring of intracellular Ca^{2+}? It is always risky to make such predictions, but my guess would point toward improved targeting of fluorescent indicators, especially by molecular genetic tricks roughly analogous to those already demonstrated for aequorin. Because fluorescent indicators give 10^3 to 10^5 more photons per molecule than aequorin can, and are not destroyed by Ca^{2+}, they will always have major advantages once they too are constructable by molecular biology. This dream is well within possibility. For example, Ca^{2+} indicators that shift emission wavelengths have been constructed (Miyawaki et al., 1997) from color-shifted mutants of the Green Fluorescent Protein (GFP) of *Aequorea victoria* (Cubitt et al., 1995b) fused to calmodulin and a calmodulin-binding peptide. Simple expression of the genetic construct synthesizes the fluorescent indicator in situ without addition of any small molecules such as coelenterazine. Such protein-based indicators are easily targeted to specific organelles (Miyawaki et al., 1997), and should be fused to other key proteins in Ca^{2+} signaling and incorporated into transgenic organisms. Such harnessing of molecular biology should answer many of today's remaining intractable questions about $[Ca^{2+}]_i$.

Acknowledgments The research in my laboratory is supported by the Howard Hughes Medical Institute and by the National Institutes of Health (NS27177).

References

Adams, S. R., Kao, J. P. Y., Grynkiewicz, G., Minta, A., and Tsien, R. Y. (1988) Biologically useful chelators that release Ca^{2+} upon illumination. *J. Am. Chem. Soc.* 110: 3212–3220.

Adams, S. R., Kao, J. P. Y., and Tsien, R.Y. (1989) Biologically useful chelators that take up Ca^{2+} upon illumination. *J. Am. Chem. Soc.* 111: 7957–7968.

Akkaya, E. U. and Lakowicz, J. R. (1993) Styryl-based wavelength-ratiometric probes: a new class of fluorescent calcium probes with long wavelength emission and a large Stokes' shift. *Anal. Biochem.* 213: 285–289.

Almers, W. and Neher, E. (1985) The Ca signal from fura-2 loaded mast cells depends strongly on the method of dye-loading. *FEBS Lett.* 192: 13–18.

Anderegg, G., Hubmann, E., Podder, N.G., and Wenk, F. (1977) Pyridinderivate als Komplexbildner. XI. Die Thermodynamik der Metallkomplexbildung mit Bis-, Tris, und Tetrakis[(2-pyridyl)methyl]-aminen. *Helv. Chim. Acta* 60: 123–140.

Arslan, P., Di Virgilio, F., Beltrame, M., Tsien, R. Y., and Pozzan, T. (1985) Cytosolic Ca^{2+} homeostasis in Ehrlich and Yoshida carcinomas. *J. Biol. Chem.* 260: 2719–2727.

Ashley, C. C., Griffiths, P. J., Lea, T. J., Mulligan, P., Palmer, R. E., and Simnett, S. J. (1991) Use of fluorescent TnC derivatives and 'caged' compounds to study cellular Ca^{2+} phenomena. In *Cellular Calcium* (McCormack, J. G. and Cobbold, P. H. eds.). Oxford, Oxford University Press, pp. 177–203.

Augustine, G. J. and Neher, E. (1992) Neuronal Ca^{2+} signalling takes the local route. *Curr. Opin. Neurobiol.* 2: 302–307.

Bacskai, B. J., Wallén, P., Lev-Ram, V., Grillner, S., and Tsien, R. Y. (1995) Activity-related calcium dynamics in lamprey motoneurons as revealed by video-rate confocal microscopy. *Neuron* 14: 19–28.

Badar-Goffer, R. S., Ben-Yoseph, O., Dolin, S. J., Morris, P. G., Smith, G. A., and Bachelard, H.S. (1990) Use of 1,2-bis(2-amino-5-fluorophenoxy)ethane-*N*, *N*, *N'*, *N'*-tetraacetic acid (5FBAPTA) in the measurement of free intracellular calcium in the brain by ^{19}F-nuclear magnetic resonance spectroscopy. *J. Neurochem.* 55: 878–884.

Bancel, F., Salmon, J. M., Vigo, J., Vo-Dinh, T., and Viallet, P. (1992) Investigation of noncalcium interactions of fura-2 by classical and synchronous fluorescence spectroscopy. *Anal. Biochem.* 204: 231–238.

Baudet, S., Hove-Madsen, L., and Bers, D.M. (1994) How to make and use calcium-specific mini- and microelectrodes. *Methods Cell Biol.* 40: 93–113.

Baumann, O., Walz, B., Somlyo, A. V., and Somlyo, A.P. (1991) Electron probe microanalysis of calcium release and magnesium uptake by endoplasmic reticulum in bee photoreceptors. *Proc. Natl. Acad. Sci. USA* 88: 741–744.

Becker, P. L. and Fay, F. S. (1987) Photobleaching of fura-2 and its effect on determination of calcium concentrations. *Am. J. Physiol.* 253: C613–C618.

Beeler, T. (1990) Oxidation of sulfhydryl groups and inhibition of the $(Ca^{2+} + Mg^{2+})$-ATPase by arsenazo III. *Biochim. Biophys. Acta* 1027: 264–267.

Belan, P. V., Gerasimenko, O. V., Tepikin, A. V., and Petersen, O.H. (1996) Localization of Ca^{2+} extrusion sites in pancreatic acinar cells. *J. Biol. Chem.* 271: 7615–7619.

Bissell, R. A., de Silva, A. P., Gunaratne, H. Q. N., Lynch, P. L. M., McCoy, C. P., Maguire, G. E. M., and Sandanayake, K. R. A. S. (1993) Fluorescent photoinduced electron-transfer sensors: the simple logic and its extensions. In *Fluorescent Chemosensors for Ion and Molecule Recognition.* (Czarnik, A. W. ed.) Washington, DC, American Chemical Society, pp. 45–58.

Blatter, L. A. and Wier, W. G. (1990) Intracellular diffusion, binding, and compartmentalization of the fluorescent calcium indictors indo-1 and fura-2. *Biophys. J.* 58: 1491–1499.

Blinks, J. R., Wier, W. G., Hess, P., and Predergast, F. G. (1982) Measurement of Ca^{2+} concentrations in living cells. *Prog. Biophys. Mol. Biol.* 40: 1 114.

Bootman, M. D., Missiaen, L., Parys, J. B., De Smedt, H., and Casteels, R. (1995) Control of inositol 1,4,5-trisphosphate-induced Ca^{2+} release by cytosolic Ca^{2+}. *Biochem. J.* 306: 445–451.

Borle, A. B. (1981) Control, modulation, and regulation of cell calcium. *Rev. Physiol. Biochem. Pharmacol.* 90: 13–153.

Brini, M., Marsault, R., Bastianutto, C., Pozzan, T., and Rizzuto, R. (1994) Nuclear targeting of aequorin. A new approach for measuring nuclear Ca^{2+} concentration in intact cells. *Cell Calcium,* 16: 259 268.

Brini, M., Marsault, R., Bastianutto, C., Alvarez, J., Pozzan, T., and Rizzuto, R. (1995) Transfected aequorin in the measurement of cytosolic Ca^{2+} concentration ($[Ca^{2+}]_c$). A critical evaluation. *J. Biol. Chem.* 270: 9896–9903.

Busa, W. B. (1992) Spectral characterization of the effect of vicosity on fura-2 fluorescence: excitation wavelength optimization abolishes the viscosity artifact. *Cell Calcium* 13: 313–319.

Button, D. and Eidsath, A. (1996) Aequorin targeted to the endoplasmic reticulum reveals heterogeneity in luminal Ca^{++} concentration and reports agonist- or $InsP_3$-induced release of Ca^{++}. *Mol. Biol. Cell* 7: 419–434.

Callaham, D. A. and Hepler, P. K. (1991) Measurement of free calcium in plant cells. In *Cellular Calcium* (McCormack, J. G. and Cobbold, P. H. eds.). Oxford, Oxford University Press, pp. 383–410.

Campbell, A. K. (1983) *Intracellular Calcium.* John Wiley and Sons, Chichester.

Campbell, A. K., Lea, T. J., and Ashley, C. C. (1979) Coelentercate photoproteins. In *Detection and Measurement of Free Ca^{2+} in Cells* (Ashley, C. C. and Campbell, A. K. eds.). Amsterdam, Elsevier, pp. 13–72.

Campbell, A. K., Trewavas, A. J., and Knight, M. R. (1996) Calcium imaging shows differential sensitivity to cooling and communication in luminous transgenic plants. *Cell Calcium* 19: 211–218.

Chandra, S., Fewtrell, C., Millard, P. J., Sandison, D. R., Webb, W. W., and Morrison, G. H. (1994) Imaging of total intracellular calcium and calcium influx and efflux in individual resting and stimulated tumor mast cells using ion microscopy. *J. Biol. Chem.* 269: 15168–15194.

Chow, R. H., Klingauf, J., and Neher, E. (1994) Time course of Ca^{2+} concentration triggering exocytosis in neuroendocrine cells. *Proc. Natl. Acad. Sci. USA* 91: 12765–12769.

Chused, T. M., Wilson, H. A., Greenblatt, D., Ishida, Y., Edison, L. J., Tsien, R. Y., and Finkelman, F.D. (1987) Flow cytometric analysis of cytosolic free calcium in murine splenic B lymphocytes: responses to anti-IgM and anti-IgD differ. *Cytometry* 8: 396–404.

Clarke, S. D., Metcalfe, J. C., and Smith, G. A. (1993) Design and properties of new ^{19}F NMR Ca^{2+} indicators: modulation of the affinities of BAPTA derivatives *via* alkylation. *J. Chem. Soc., Perkin Trans.* 2: 1187–1209.

Cobbold, P. H. and Lee, J. A. C. (1991) Aequorin measurements of cytoplasmic free calcium. In *Cellular Calcium* (McCormack, J. G. and Cobbold, P. H. eds.) Oxford, Oxford University Press, pp. 55–81.

Cobbold, P. H. and Rink, T. J. (1987) Fluorescence and bioluminescence measurement of cytoplasmic free calcium. *Biochem. J.* 248: 313–328.

Combettes, L., Champeil, P., Finch, E. A., and Goldin, S. M. (1994) Calcium and inositol 1,4,5-trisphosphate-induced Ca^{2+} release. *Science* 265: 813–815.

Connor, J. A. (1994) Dissecting signals from fura-2 in cytosol, nucleus, and other organelles in living cells. *Neuroprotocols* 5: 25–34.

Cubitt, A. B., Firtel, R. A., Fischer, G., Jaffe, L. F., and Miller, A. L. (1995a) Patterns of free calcium in multicellular stages of Dictyostelium expressing jellyfish aequorin. *Development* 121: 2291–2301.

Cubitt, A. B., Heim, R., Adams, S. R., Boyd, A. E., Gross, L. A., and Tsien, R. Y. (1995b) Understanding, using and improving green fluorescent protein. *Trends Biochem. Sci.* 20: 448–455.

DeMarinis, R. M., Katerinopoulos, H. E., and Muirhead, K. A. (1990) New tetracarboxylate compounds as fluorescent intracellular calcium indicators. *Biochem. Methods* 112: 381

Denk, W., Holt, J. R., Shepherd, G. M., and Corey, D. P. (1995) Calcium imaging of single stereocilia in hair cells: localization of transduction channels at both ends of tip links. *Neuron* 15: 1311–1321.

Di Virgilio, F., Steinberg, T. H., Swanson, J. A., and Silverstein, S.C. (1988) Fura-2 secretion and sequestration in macrophages. *J. Immunol.* 140: 915–920.

Docampo, R., Moreno, S. N. J., and Mason, R. P. (1993) Generation of free radical metabolites and superoxide anion by the calcium indicators arsenazo III, antipyrylazo III, and murexide in rat liver microsomes. *J. Biol. Chem.* 258: 14920–14925.

Duchen, M. R. (1992) Fluorescence—monitoring cell chemistry *in vivo*. In *Monitoring Neuronal Activity* (Stamford, J. A. ed.). Oxford, Oxford University Press, pp. 231–260.

Eberhard, M. and Erne, P. (1991) Calcium binding to fluorescent calcium indicators: calcium green, calcium orange and calcium crimson. *Biochem. Biophys. Res. Commun.* 180: 209–215.

Ferres, H. (1980) Pro-drugs of β-lactam antibiotics. *Chem. Ind.* 435–440.

Garcia-Sancho, J. (1984) Inhibition of glycolysis in the human erythrocyte by formaldehyde and Ca-chelator esters. *J. Physiol.* 357: 60P.

Gerig, J. T., Singh, P., Levy, L. A., and London, R. E. (1987) Calcium complexation with a highly calcium selective chelator: crystal structure of Ca(CaFBAPTA)·5H_2O. *J. Inorg. Biochem.* 31: 113–121.

Grohovaz, F., Bossi, M., Pezzati, R., Meldolesi, J., and Tarelli, F.T. (1996) High resolution ultrastructural mapping of total calcium: electron spectroscopic imaging/electron energy loss spectroscopy analysis of a physically/chemically processed nerve-muscle preparation. *Proc. Natl. Acad. Sci. USA* 93: 4799–4803.

Grynkiewicz, G., Poenie, M., and Tsien, R.Y. (1985) A new generation of Ca^{2+} indicators with greatly improved fluorescence properties. *J. Biol. Chem.* 260: 3440–3450.

Hahn, K., DeBiasio, R., and Taylor, D. L. (1992) Patterns of elevated free calcium and calmodulin activation in living cells. *Nature* 359: 736–738.

Hajnóczky, G., Robb-Gaspers, L. D., Seitz, M. B., and Thomas, A. P. (1995) Decoding of cytosolic calcium oscillations in the mitochondria. *Cell* 82: 415 424.

Hallam, T. J. and Rink, T. J. (1985) Agonists stimulate divalent cation channels in the plasma membrane of human platelets. *FEBS Lett.* 186: 175–179.

Harding, D. P., Smith, G. A., Metcalfe, J. C., Morris, P. G., and Kirschenlohr, H. L. (1993) Resting and end-diastolic $[Ca^{2+}]_i$ measurements in the Langendorff-perfused ferret heart loaded with ^{19}F NMR indicator. *Magn. Reson. Med.* 29: 605–615.

Haugland, R. P. (1996) *Handbook of Fluorescent Probes and Research Chemicals*, 6th edn. Molecular Probes, Eugene, OR.

Hesketh, T. R., Smith, G. A., Moore, J. P., Taylor, M. W., and Metcalfe, J.C. (1983) Free cytoplasmic calcium concentration and the mitogenic stimulation of lymphocytes. *J. Biol. Chem.* 258: 4876–4882.

Hinkle, P. M., Shanshala, E. D. II, and Nelson, E. J. (1992) Measurement of intracellular cadmium with fluorescent dyes. Further evidence for the role of calcium channels in cadmium uptake. *J. Biol. Chem.* 267: 25553–25559.

Hirota, A., Chandler, W. K., Southwick, P. L., and Waggoner, A.S. (1989) Calcium signals recorded from two new purpurate indicators inside frog cut twitch fibers. *J. Gen. Physiol.* 94: 597–631.

Hofer, A. M. and Machen, T. E. (1993) Technique for *in situ* measurement of calcium in intracellular inositol 1,4,5-trisphosphate-sensitive stores using the fluorescent indicator mag-fura-2. *Proc. Natl. Acad. Sci. USA* 90: 2598–2602.

Hofer, A. M. and Schulz, I. (1996) Quantification of intraluminal free [Ca] in the agonist-sensitive internal calcium store using compartmentalized fluorescent indicators: some considerations. *Cell Calcium* 20: 235–242.

Hofer, A. M., Fasolato, C., and Pozzan, T. (1998) Capacitative Ca^{2+} entry is closely linked to the filling state of internal Ca^{2+} stores: a study using simultaneous measurements of I_{CRAC} and intraluminal $[Ca^{2+}]$. *J. Cell Biol.* 140: 325–334.

Homolya, L., Hollo, Z., Germann, U. A., Pastan, I., Gottesman, M. M., and Sarkadi, B. (1993) Fluorescent cellular indicators are extruded by the multidrug resistance protein. *J. Biol. Chem.* 268: 21493–21496.

Horne, J. H. and Meyer, T. (1995) Luminal calcium regulates the inositol trisphosphate receptor of rat basophilic leukemia cells at a cystolic site. *Biochemistry* 34: 12738–12746.

Huston, M. E., Haider, K. W., and Czarnik, A.W. (1988) Chelation-enhanced fluorescence in 9,10-bis(TMEDA)anthracene. *J. Am. Chem. Soc.* 110: 4460–4462.

Iatridou, H., Foukaraki, E., Kuhn, M. A., Marcus, E. M., Haugland, R. P., and Katerinopoulos, H.E. (1994) The development of a new family of intracellular calcium probes. *Cell Calcium* 15: 190–198.

Jansen, A. B. A. and Russell, T. J. (1965) Some novel penicillin derivatives. *J. Chem. Soc.* 2127–2132.

Jefferson, J. R., Hunt, J. B., and Ginsburg, A. (1990) Characterization of indo-1 and quin-2 as spectroscopic probes for Zn^{2+}-protein interactions. *Anal. Biochem.* 187: 328 336.

Jong, D. S., Pape, P. C., Baylor, S. M., and Chandler, W. K. (1995) Calcium inactivation of calcium release in frog cut muscle fibers that contain millimolar EGTA or fura-2. *J. Gen. Physiol.* 106: 337–388.

Kao, J. P. Y. (1994) Practical aspects of measuring $[Ca^{2+}]$ with fluorescent indicators. *Methods Cell Biol.* 40: 155–181.

Kao, J. P. Y. and Tsien, R. Y. (1988) Ca^{2+} binding kinetics of fura-2 and azo-1 from temperature-jump relaxation measurements. *Biophys. J.* 53: 635–639.

Kao, J. P. Y., Harootunian, A. T., and Tsien, R. Y. (1989) Photochemically generated cytosolic calcium pulses and their detection by fluo-3. *J. Biol. Chem.* 264: 8179–8184.

Kao, J. P. Y., Alderton, J. M., Tsien, R. Y., and Steinhardt, R. A. (1990) Active involvement of Ca^{2+} in mitotic progression of Swiss 3T3 fibroblasts. *J. Cell Biol.* 111: 183–196.

Kawanishi, T., Blank, L. M., Harootunian, A. T., Smith, M. T., and Tsien, R. Y. (1989) Ca^{2+} oscillations induced by hormonal stimulation of individual fura-2-loaded hepatocytes. *J. Biol. Chem.* 264: 12859–12866.

Kendall, J. M., Badminton, M. N., Sala-Newby, G. B., Campbell, A. K., and Rembold, C. M. (1996) Recombinant apoaequorin acting as a pseudo-luciferase reports micromolar changes in the endoplasmic reticulum free Ca^{2+} of intact cells. *Biochem. J.* 318: 383–387.

Konishi, M., Olson, A., Hollingworth, S., and Baylor, S. M. (1988) Myoplasmic binding of fura-2 investigated by steady-state fluorescence and absorbance measurements. *Biophys. J.* 54: 1089–1104.

Kudo, Y., Nakamura, T., and Ito, E. (1991) A 'macro' image analysis of fura-2 fluorescence to visualize the distribution of functional glutamate receptor sybtypes in hippocampal slices. *Neurosci. Res.* 12: 412–420.

Kuhn, M. A. (1993) 1,2-Bis(2-aminophenoxy)ethane-*N,N,N′,N′*-tetraacetic acid conjugates used to measure intracellular Ca^{2+} concentration. In *Fluorescent Chemosensors for Ion Molecule Recognition.* (Czarnik, A. W. ed.). Washington, DC, American Chemical Society, pp. 147–161.

Lakowicz, J. R., Szmacinski, H., and Johnson, M. L. (1992a) Calcium imaging using fluorescence lifetimes and long-wavelength probes. *J. Fluoresc.* 2: 47–62.

Lakowicz, J. R., Szmacinski, H., Nowaczyk, K., and Johnson, M. L. (1992b) Fluorescence lifetime imaging of calcium using quin-2. *Cell Calcium* 13: 131–147.

Lakowicz, J. R., Szmacinski, H., Nowaczyk, K., Lederer, W. J., Kirby, M. S., and Johnson, M. L. (1994) Fluorescence lifetime imaging of intracellular calcium in COS cells using quin-2. *Cell Calcium* 15: 7–27.

Lattanzio, F. A. Jr. and Bartschat, D. K. (1991) The effect of pH on rate constants, ion selectivity and thermodynamic properties of fluorescent calcium and magnesium indicators. *Biochem. Biophys. Res. Commun.* 177: 184–191.

Levy, L. A., Murphy, E., Raju, B., and London, R. E. (1988) Measurement of cytosolic free magnesium ion concentration by ^{19}F NMR. *Biochemistry* 27: 4041–4048.

Lew, V. L., Tsien, R. Y., Miner, C., and Bookchin, R. M. (1982) Physiological $[Ca^{2+}]_i$ level and pump-leak turnover in intact red cells measured using an incorporated Ca chelator. *Nature* 298: 478–481.

Llinás, R., Sugimori, M., and Silver, R. B. (1992) Microdomains of high calcium concentration in a presynaptic terminal. *Science* 256: 677–679.

Lloyd, Q. P., Kuhn, M. A., and Gay, C. V. (1995) Characterization of calcium translocation across the plasma membrane of primary osteoblasts using a lipophilic calcium-sensitive fluorescent dye, calcium green C_{18}. *J. Biol. Chem.* 270: 22445–22451.

Lojewska, Z. and Loew, L. M. (1987) Insertion of amphiphilic molecules into membranes is catalyzed by a high molecular weight non-ionic surfactant. *Biochim. Biophys. Acta* 899: 104–112.

London, R. E., Rhee, C. K., Murphy, E., Gabel, S., and Levy, L.A. (1994) NMR-sensitive fluorinated and fluorescent intracellular calcium ion indicators with high dissociation constants. *Am. J. Physiol.* 266: C1313–C1322.

Malgaroli, A., Milani, D., Meldolesi, J., and Pozzan, T. (1987) Fura-2 measurement of cytosolic free Ca^{2+} in monolayers and suspensions of various types of animal cells. *J. Cell Biol.* 105: 2145–2155.

McClellan, A. D., McPherson, D., and O'Donovan, M. J. (1994) Combined retrograde labeling and calcium imaging in spinal cord and brainstem neurons of the lamprey. *Brain Res.* 663: 61–68.

Merritt, J. E., McCarthy, S. A., Davies, M. P. A., and Moores, K. E. (1990) Use of fluo-3 to measure cytosolic Ca^{2+} in platelets and neutrophils: loading cells with the dye, calibration of traces, measurements in the presence of plasma, and buffering of cytosolic Ca^{2+}. *Biochem. J.* 269: 513–519.

Metcalfe, J. C. and Smith, G. A. (1991) NMR measurement of cytoplasmic free calcium concentration by fluorine labelled indicators. In *Cellular Calcium* (McCormack, J. G. and Cobbold, P. H. eds.), Oxford, Oxford University Press, pp. 123–132.

Miller, A. L., Karplus, E., and Jaffe, L. F. (1994) Imaging $[Ca^{2+}]_i$ with aequorin using a photon imaging detector. *Methods Cell Biol.* 40: 305–338.

Miller, D. L. and Korenbrot, J. I. (1987) Kinetics of light-activated Ca fluxes across the plasma membrane of rod outer segments: a dynamic model of the regulation of cytoplasmic Ca concentration. *J. Gen. Physiol.* 90: 397–425.

Minta, A., Kao, J. P. Y., and Tsien, R. Y. (1989) Fluorescent indicators for cytosolic calcium based on rhodamine and fluorescein chromophores. *J. Biol. Chem.* 264: 8171–8178.

Miyawaki, A., Llopis, J., Heim, R., McCaffery, J. M., Adams, J. A., Ikura, M., and Tsien, R. Y. (1997) Fluorescent indicators for Ca^{2+} based on green fluorescent proteins and calmodulin. *Nature* 388: 882–887.

Montero, M., Brini, M., Marsault, R., Alvarez, J., Sitia, R., Pozzan, T., and Rizzuto, R. (1995) Monitoring dynamic changes in free Ca^{2+} concentration in the endoplasmic reticulum of intact cells. *EMBO J.* 14: 5467–5475.

Moreton, R. B. (1991) Optical techniques and Ca^{2+} imaging. In *Cellular Neurobiology* (Chad, J. and Wheal, H. eds.). Oxford, Oxford University Press, pp. 205–222.

Nakajima-Shimada, J., Iida, H., Tsuji, F. I., and Anraku, Y. (1991) Monitoring of intracellular calcium in *Saccharomyces cerevisiae* with an apoaequorin cDNA expression system. *Proc. Natl. Acad. Sci. USA* 88: 6878–6882.

Neher, E. (1986) Concentration profiles of intracellular calcium in the presence of a diffusible chelator. *Exp. Brain Res.* 14: 80–96.

Nowycky, M. C. and Pinter, M. J. (1993) Time courses of calcium and calcium-bound buffers following calcium influx in a model cell. *Biophys. J.* 64: 77–91.

Orchard, C. H., Boyett, M. R., Fry, C. H., and Hunter, M. (1991) The use of electrodes to study cellular Ca^{2+} metabolism. In *Cellular Calcium: A Practical Approach* (McCormack, J. G. and Cobbold, P. H. eds.). Oxford, Oxford University Press, pp. 83–113.

Patel, S. and Taylor, C. W. (1995) Quantal responses to inositol 1,4,5-trisphosphate are not a consequence of Ca^{2+} regulation of inositol 1,4,5-trisphosphate receptors. *Biophys. J.* 312: 789–794.

Penner, R., Matthews, G., and Neher, E. (1988) Regulation of calcium influx by second messengers in rat mast cells. *Nature* 334: 499–504.

Perrin, D. D., Dempsey, B., and Serjeant, E. P. (1981) *pK_a Prediction for Organic Acids and Bases.* Chapman and Hall, New York.

Pethig, R., Kuhn, M., Payne, R., Adler, E., Chen, T.-H., and Jaffe, L. F. (1989) On the dissociation constants of BAPTA-type calcium buffers. *Cell Calcium* 10: 491–498.

Poenie, M. (1992) Measurement of intracellular calcium with fluorescent calcium indicators. In *Neuromethods vol. 20: Intracellular Messengers*, (Boulton, A., Baker, G., and Taylor, C. eds.). Humana Press, Totowa, NJ, pp. 129–170.

Poenie, M., Alderton, J., Steinhardt, R., and Tsien, R. (1986) Calcium rises abruptly and briefly throughout the cell at the onset of anaphase. *Science* 233: 886–889.

Quast, U., Labhardt, A. M., and Doyle, V. M. (1984) Stopped-flow kinetics of the interaction of the fluorescent calcium indicator quin-2 with calcium ions. *Biochem. Biophys. Res. Commun.* 123: 604–611.

Raju, B., Murphy, E., Levy, L. A., Hall, R. D., and London, R. E. (1989) A fluorescent indicator for measuring cytosolic free magnesium. *Am. J. Physiol.* 256: C540- C548.

Ranganathan, R., Bacskai, B. J., Tsien, R. Y., and Zuker, C. S. (1994) Cytosolic calcium transients: spatial localization and role in *Drosophila* photoreceptor cell function. *Neuron* 13: 837–848.

Ratto, G. M., Payne, R., Owen, W. G., and Tsien, R. Y. (1988) The concentration of cytosolic free calcium in vertebrate rod outer segments measured with fura-2. *J. Neurosci.* 8: 3240–3246.

Regehr, W. G. and Tank, D. W. (1991) Selective fura-2 loading of presynaptic terminals and nerve cell processes by local perfusion in mammalian brain slice. *J. Neurosci. Methods* 37: 111–119.

Rettig, W. (1986) Charge separation in excited states of decoupled systems—TICT compounds and implications regarding the development of new laser dyes and the primary processes of vision and photosynthesis. *Angew. Chem., Int. Ed. Engl.* 25: 971–988.

Rizzuto, R., Bastianutto, C., Brini, M., Murgia, M., and Pozzan, T. (1994a) Mitochondrial Ca^{2+} homeostasis in intact cells. *J. Cell Biol.* 126: 1183–1194.

Rizzuto, R., Brini, M., and Pozzan, T. (1994b) Targeting recombinant aequorin to specific intracellular organelles. *Methods Cell Biol.* 40: 339–358.

Robitaille, P. M. and Jiang, Z. (1992) New calcium-sensitive ligand for nuclear magnetic resonance spectroscopy. *Biochemistry* 31: 12585–12591.

Rutter, G. A., Burnett, P., Rizzuto, R., Brini, M., Murgia, M., Pozzan, T., Tavare, J. M., and Denton, R. M. (1996) Subcellular imaging of intramitochondrial Ca^{2+} with recombinant targeted aequorin: significance for the regulation of pyruvate dehydrogenase activity. *Proc. Natl. Acad. Sci. USA* 93: 5489–5494.

Sanders, R. (1995) Fluorescence lifetime as a contrast mechanism in confocal imaging. Ph.D. thesis, Universiteit Utrecht.

Sanui, H. and Rubin, H. (1982) Atomic absorption measurement of cations in cultured cells. In *Ions, Cell Proliferation, and Cancer.* (Boynton, A. L., McKeehan, W. L., and Whitfield, J. F. eds.). Academic Press, New York, pp. 41–52.

Scheenen, W. J. J. M., Makings, L. R., Gross, L.R ., Pozzan, T., and Tsien, R. Y. (1996) Photodegradation of indo-1 and its effect on apparent Ca^{2+} concentrations. *Chem. Biol.* 3: 765–774.

Schilling, W. P., Rajan, L., and Strobl-Jager, E. (1989) Characterization of the bradykinin-stimulated calcium influx pathway of cultured vascular endothelial cells. Saturability, selectivity, and kinetics. *J. Biol. Chem.* 264: 12838–12848.

Schneggenburger, R., Zhou, Z., Konnerth, A., and Neher, E. (1993) Fractional contribution of calcium to the cation current through glutamate receptor channels. *Neuron* 11: 133–143.

Shibuya, I. and Douglas, W. W. (1992) Calcium channels in rat melanotrophs are permeable to manganese, cobalt, cadmium, and lanthanum, but not to nickel: evidence provided by fluorescence changes in fura-2 loaded cells. *Endocrinology* 131: 1936–1941.

Shimomura, O. (1995) Luminescence of aequorin is triggered by the binding of two calcium ions. *Biochem. Biophys. Res. Commun.* 211: 359–363.

Shimomura, O., Musicki, B., Kishi, Y., and Inouye, S. (1993) Light-emitting properties of recombinant semi-synthetic aequorins and recombinant fluorescein-conjugated aequorin for measuring cellular calcium. *Cell Calcium* 14: 373–378.

Short, A. D., Klein, M. G., Schneider, M. F., and Gill, D. L. (1993) Inositol 1,4,5-trisphosphate-mediated quantal Ca^{2+} release measured by high resolution imaging of Ca^{2+} within organelles. *J. Biol. Chem.* 268: 25887–25893.

Smith, G. A., Metcalfe, J. C., and Clarke, S. D. (1993) The design and properties of a series of calcium indicators which shift from rhodamine-like to fluorescein-like fluorescence on binding calcium. *J. Chem. Soc., Perkin Trans.* 2: 1195–1204.

Smith, P. J. S., Sanger, R. H., and Jaffe, L. F. (1994) The vibrating Ca^{2+} electrode: a new technique for detecting plasma membrane regions of Ca^{2+} influx and efflux. *Methods Cell Biol.* 40, 115–134.

Somlyo, A. V., Bond, M., Broderick, R., and Somlo, A .P. (1988) Calcium and magnesium movements through sarcoplasmic reticulum, endoplasmic reticulum, and mitochondria. *Adv. Exp. Med. Biol.* 232: 221–229.

Speksnijder, J. E., Miller, A. L., Weisenseel, M. H., Chen, T.-H., and Jaffe, L. F. (1989) Calcium buffer injections block fucoid egg development by facilitating calcium diffusion. *Proc. Natl. Acad. Sci. USA* 86: 6607–6611.

Spray, D. C., Nerbonne, J., Campos de Carvalho, A., Harris, A. L., and Bennett, M. V. L. (1984) Substituted benzyl acetates: a new class of compounds that reduce gap junctional conductance by cytoplasmic acidification. *J. Cell Biol.* 99: 174–179.

Szmacinski, H. and Lakowicz, J. R. (1995) Possibility of simultaneously measuring low and high calcium concentrations using fura-2 and lifetime-based sensing. *Cell Calcium* 18: 64–75.

Szmacinski, H., Gryczynski, I., and Lakowicz, J.R. (1993) Calcium-dependent fluorescence lifetimes of indo-1 for one- and two-photon excitation of fluorescence. *Photochem. Photobiol.* 58: 341–345.

Tepikin, A. V., Llopis, J., Snitsarev, V. A., Gallacher, D. V., and Petersen, O. H. (1994) The droplet technique: measurement of calcium extrusion from single isolated mammalian cells. *Pflügers Arch.* 428: 664–670.

Thomas, A. P. and Delaville, F. (1991) The use of fluorescent indicators for measurements of cytosolic-free calcium concentration in cell populations and single cells. In *Cellular Calcium* (McCormack, J. G. and Cobbold, P. H. eds.). Oxford University Press, Oxford, pp. 1 54.

Thomas, M. V. (1982) *Techniques in Calcium Research.* Academic Press, New York.

Thomas, M. V. (1991) Metallochromic indicators. In *Cellular Calcium*, (McCormack, J. G. and Cobbold, P. H. eds.). Oxford University Press, Oxford, pp. 115–122.

Tomsig, J. L. and Suszkiw, J. B. (1990) Pb^{2+}-induced secretion from bovine chromaffin cells: fura-2 as a probe for Pb^{2+}. *Am. J. Physiol.* 259: C762–C768.

Tran, N. N. P., Leroy, P., Bellucci, L., Robert, A., Nicolas, A., Atkinson, J., and Capdeville-Atkinson, C. (1995) Intracellular concentrations of fura-2 and fura-2/AM in vascular smooth muscle cells following perfusion loading of fura-2/AM in arterial segments. *Cell Calcium* 18: 420–428.

Trezl, L., Rusznak, I., Tyihak, E., Szarvas, T., and Szende, B. (1983) Spontaneous N^{ϵ}-methylation and N^{ϵ}-formylation reactions between L-lysine and formaldehyde inhibited by L-ascorbic acid. *Biophys. J.* 214: 289 292.

Tse, F. W. and Hille, B. (1994) Cyclic Ca^{2+} changes in intracellular stores of gonadotropes during gonadotropin-releasing hormone-stimulated Ca^{2+} oscillations. *Proc. Natl. Acad. Sci. USA* 91: 9750–9754.

Tsien, R. Y. (1980) New calcium indicators and buffers with high selectivity against magnesium and protons: design, synthesis, and properties of prototype structures. *Biochemistry* 19: 2396–2404.

Tsien, R. Y. (1981) A non-disruptive technique for loading calcium buffers and indicators into cells. *Nature* 290: 527–528.

Tsien, R. Y. (1983) Intracellular measurements of ion activities. *Annu. Rev. Biophys. Bioeng.* 12: 94–116.

Tsien, R. Y. (1988) Fluorescent measurement and photochemical manipulation of cytosolic free calcium. *Trends Neurosci.* 11: 419–424.

Tsien, R. Y. (1989a) Fluorescent indicators of ion concentrations. *Methods Cell Biol.* 30: 127–156.

Tsien, R. Y. (1989b) Fluorescent probes of cell signaling. *Annu. Rev. Neurosci.* 12: 227–253.

Tsien, R.Y. (1992) Intracellular signal transduction in four dimensions: from molecular design to physiology (1992 Bowditch Lecture). *Am. J. Physiol.* 263: C723 - C728.

Tsien, R. Y. (1993) Fluorescent and photochemical probes of dynamic biochemical signals inside living cells. In *Fluorescent Chemosensors for Ions and Molecule Recognition.* (Czarnik, A. W. ed.). pp. 130–146. American Chemical Society, Columbus, OH, pp. 130–146.

Tsien, R. Y. and Bacskai, B. J. (1995) Video-rate confocal microscopy. In *Handbook of Biological Confocal Microscopy.* 2nd edn. (Pawley, J. B. ed.). Plenum Press, New York, pp. 459–478.

Tsien, R. Y. and Poenie, M. (1986) Fluorescence ratio imaging: a new window into intracellular ionic signaling. *Trends Biochem. Sci.* 11: 450–455.

Tsien, R. Y. and Pozzan, T. (1989) Measurement of cytosolic free Ca^{2+} with quin2: practical aspects. *Methods Enzymol.* 172: 230–262.

Tsien, R. Y. and Rink, T.J. (1983) Measurement of cytoplasmic free Ca^{2+}. In *Current Methods of Cellular Neurobiology*, 3rd edn. (Barker, J. and McKelvey, J. F. eds.). Wiley, New York.

Tsien, R. Y., Pozzan, T., and Rink, T.J. (1982) Calcium homeostasis in intact lymphocytes: cytoplasmic free Ca^{2+} monitored with a new, intracellularly trapped fluorescent indicator. *J. Cell Biol.* 94: 325–334.

Tymianski, M., Wallace, M. C., Spigelman, I., Uno, M., Carlen, P. L., Tator, C. H., and Charlton, M. P. (1993) Cell-permeant Ca^{2+} chelators reduce early excitotoxic and ischemic neuronal injury *in vitro* and *in vivo*. *Neuron* 11: 221–235.

Tymianski, M., Spigelman, I., Zhang, L., Carlen, P. L., Tator, C. H., Charlton, M. P., and Wallace, M. C. (1994) Mechanism of action and persistence of neuroprotection by cell-permeant Ca^{2+} chelators. *J. Cereb. Blood Flow Metab.* 14: 911–923.

Vorndran, C., Minta, A., and Poenie, M. (1995) New fluorescent calcium indicators designed for cytosolic retention or measuring calcium near membranes. *Biophys. J.* 69: 2112–2124.

Wendt-Gallitelli, M. F. and Isenberg, G. (1991) X-ray microanalysis. In *Cellular Calcium: A Practical Approach.* (McCormack, J. G. and Cobbold, P. H. eds.). Oxford University Press, Oxford, pp. 133–157.

Westerblad, H. and Allen, D. G. (1994) Methods for calibration of fluorescent calcium indicators in skeletal muscle fibers. *Biophys. J.* 66: 926–928.

Williams, D. A. and Fay, F. S. (1990) Imaging of cell calcium: collected papers and reviews. *Cell Calcium* 11: 55–249.

Wu, L. G. and Saggau, P. (1994) Presynaptic calcium is increased during normal synaptic transmission and paired-pulse facilitation, but not in long-term potentiation in area CA1 of hippocampus. *J. Neurosci.* 14: 645–654.

Xu, C. and Webb, W. W. (1996) Measurement of two-photon excitation cross sections of molecular fluorophores with data from 690 to 1050 nm. *J. Opt. Soc. Am. B* 13: 481 491.

Xu, C., Ziipfel, W., Shear, J. B., Williams, R. M., and Webb, W. W. (1996) Multiphoton fluorescence excitation: new spectral windows for biological nonlinear microscopy. *Proc. Natl. Acad. Sci. USA* 93: 10763–10768.

Yau, K. W. and Nakatani, K. (1984) Electrogenic Na–Ca exchange in retinal rod outer segment. *Nature* 311: 661–663.

Yuste, R. and Katz, L. C. (1991) Control of postsynaptic Ca^{2+} influx in developing neocortex by excitatory and inhibitory neurotransmitters. *Neuron* 6: 333–344.

Zhao, M., Hollingworth, S., and Baylor, S. M. (1996) Properties of tri- and tetracarboxylate Ca^{2+} indicators in frog skeletal muscle fibers. *Biophys. J.* 70: 896–916.

Zucker, R. S. (1992) Effects of photolabile calcium chelators on fluorescent calcium indicators. *Cell Calcium* 13: 29–40.